Zoned chondrules in Semarkona: Evidence for high- and low-temperature processing

JEFFREY N. GROSSMAN[1]*, CONEL M. O'D. ALEXANDER[2], JIANHUA WANG[2] AND ADRIAN J. BREARLEY[3]

[1]U.S. Geological Survey, 954 National Center, Reston, Virginia 20192, USA
[2]Department of Terrestrial Magnetism, Carnegie Institution of Washington, 5241 Broad Branch Road, NW, Washington, D.C. 20015, USA
[3]Department of Earth and Planetary Sciences, University of New Mexico, Albuquerque, New Mexico 87131, USA
*Correspondence author's e-mail address: jgrossman@usgs.gov

Abstract–At least 15% of the low-FeO chondrules in Semarkona (LL3.0) have mesostases that are concentrically zoned in Na, with enrichments near the outer margins. We have studied zoned chondrules using electron microprobe methods (x-ray mapping plus quantitative analysis), ion microprobe analysis for trace elements and hydrogen isotopes, cathodoluminescence imaging, and transmission electron microscopy in order to determine what these objects can tell us about the environment in which chondrules formed and evolved.

Mesostases in these chondrules are strongly zoned in all moderately volatile elements and H (interpreted as water). Calcium is depleted in areas of volatile enrichment. Titanium and Cr generally decrease toward the chondrule surfaces, whereas Al and Si may either increase or decrease, generally in opposite directions to one another; Mn follows Na in some chondrules but not in others; Fe and Mg are unzoned. D/H ratios increase in the water-rich areas of zoned chondrules. Mesostasis shows cathodoluminescence zoning in most zoned chondrules, with the brightest yellow color near the outside. Mesostasis in zoned chondrules appears to be glassy, with no evidence for devitrification.

Systematic variations in zoning patterns among pyroxene- and olivine-rich chondrules may indicate that fractionation of low- and high-Ca pyroxene played some role in Ti, Cr, Mn, Si, Al, and some Ca zoning. But direct condensation of elements into hot chondrules, secondary melting of late condensates into the outer portions of chondrules, and subsolidus diffusion of elements into warm chondrules cannot account for the sub-parallel zoning profiles of many elements, the presence of H_2O, or elemental abundance patterns.

Zoning of moderately volatile elements and Ca may have been produced by hydration of chondrule glass without devitrification during aqueous alteration on the parent asteroid. This could have induced structural changes in the glass allowing rapid diffusion and exchange of elements between altered glass and surrounding matrix and rim material. Calcium was mainly lost during this process, and other nonvolatile elements may have been mobile as well. Some unzoned, low-FeO chondrules appear to have fully altered mesostasis.

INTRODUCTION

Understanding the origin of chondrules is one of the most challenging problems in meteoritics. Chondrules are often used to provide critical constraints on models for the solar nebula because they are widely believed to predate the formation of large bodies in the solar system. If, alternatively, chondrules formed on the surfaces of early asteroidal bodies, then chondrules could provide equally important constraints on models for the formation and evolution of those bodies. In order to use chondrules to provide constraints on any aspect of the early solar system, it is necessary to be able to disentangle their primary properties from those that were produced later by alteration. We define the "primary" composition of a chondrule to be that at the onset of crystallization following the event which caused melting for the first time.

There are many stages in the history of a chondrule when chemical and/or mineralogical (and/or isotopic) alteration could occur. (A) A partially molten chondrule may experience evaporation, condensation, or assimilation of accreted material during crystallization. (B) A recently solidified chondrule may interact with its surroundings *via* subsolidus reactions with gas while it is still in the environment in which it formed (if water vapor were involved in such reactions, the process would be a type of aqueous alteration). After a chondrule leaves the low-density environment in which it formed and comes into close proximity with other chondrules and matrix (*i.e.*, accretion to a parent body in a nebular model, or burial in an asteroidal

model), processes such as (C) aqueous alteration (involving either liquid water or vapor) and (D) thermal metamorphism may occur, with attendant transport of elements across chondrule boundaries. (E) Shock events on a parent body may create transient vapors with which chondrules can react, and may physically inject mobile phases into chondrules along cracks. (F) At any time in its history, a chondrule may be remelted. At this point, material accreted to the chondrule's surface may be incorporated into a new generation of liquid. All of this potential, indeed likelihood, for secondary modification of chondrules renders them extremely complicated systems, and makes even more difficult the task of understanding chondrule origins with little first-hand knowledge of their parent asteroids.

Secondary processing of chondrules, even in relatively unmetamorphosed chondrites, is well-documented in the literature. Dodd (1971) discovered that many chondrules in Sharps (H3.4) display non-igneous zoning of olivine, where grains near the chondrule surface are different in composition from those in the chondrule core, without regard to individual grain boundaries. It is these objects that we term *zoned chondrules* in the present paper, that is, cases where phases are zoned with respect to the chondrule surface (or with respect to some other feature not related to the igneous growth-surfaces of minerals, such as cracks). In Sharps, many of the zoned chondrules almost certainly originated by partial equilibration of chondrule olivine with more ferroan olivine in the surrounding matrix during light thermal metamorphism (*i.e.*, in environment (D) listed above). Similar thermal metamorphic effects, including changes in both olivine and chondrule mesostasis composition, have since been abundantly documented by McCoy *et al.* (1991), Sears (*e.g.*, Sears *et al.*, 1995), and others, especially in the unequilibrated ordinary chondrites (UOCs). Aqueous alteration (environment (C), or perhaps (B)) has affected chondrules in virtually every UOC and most carbonaceous chondrites, with effects ranging from the dissolution of mesostasis in fine-grained chondrules (Grossman *et al.*, 2000, and references cited therein), to formation of minor secondary minerals (*e.g.*, Hutchison *et al.*, 1987, 1994; Wasson and Krot, 1994), to the complete replacement of glass (and, in extreme cases, mafic phases) by phyllosilicates in CM and many CR chondrites.

There is comparatively little evidence for alteration of chondrules in environments (A) and (B) (*i.e.*, prior to incorporation or burial in the parent body) and much of this is controversial. Ferroan rims around olivine at the surface of some chondrules in carbonaceous and ordinary chondrites have been ascribed to subsolidus alteration by nebular gas (Peck and Wood, 1987; Pale and Fegley, 1990; Weinbruch *et al.*, 1990), although this interpretation has been disputed (*e.g.*, Wasson and Krot, 1994; Krot *et al.*, 1995, 1997a). Bridges *et al.* (1997) described metasomatism involving alkalis and chlorine in UOC chondrules, and concluded that this occurred while the chondrules were partially molten, probably following

formation on a parent body. We have questioned this interpretation (Grossman *et al.*, 2000), and think the effect is more likely to be subsolidus alteration. Ikeda and Kimura (1995a,b) described the alteration of mesostasis in chondrules from oxidized CV3 chondrites, and concluded that gas-solid reactions involving solid chondrules in the solar nebula caused an influx of alkalis and loss of Ca; but, these features can also be interpreted as the results of parent-body aqueous alteration (Krot *et al.*, 1995).

Another report of secondary processes affecting chondrules while they were still hot was published by Matsunami *et al.* (1993), and supplemented by Lyon *et al.* (1999) and Sears *et al.* (1999), who found a chondrule in Semarkona (LL3.0) with concentrically zoned mesostasis. The mesostasis in the outermost zone of this chondrule is enriched in volatile elements. The authors concluded that volatiles, lost by evaporation during chondrule formation, recondensed onto this chondrule, and subsequently diffused into the interior (environment (A) or (B)). Unlike the previously mentioned evidence of secondary processing at high temperatures, there does not appear to be any straightforward way of explaining Matsunami's zoned chondrule through parent-body processing. An abstract by Nagahara *et al.* (1999) discusses two more zoned Semarkona chondrules, and interprets their compositional gradients as the product of direct condensation of major elements to liquid during crystallization (environment (A)), followed by subsolidus entry of alkalis and inward diffusion along the same lines outlined by Matsunami *et al.* (1993). Interpretations such as these can help constrain the mechanism of chondrule formation and the environment in which they formed. Because of this great potential significance, further systematic work on a larger number of zoned chondrules is clearly required.

We report here on the first systematic study of zoned chondrules as a class. Semarkona was chosen as the host chondrite to avoid the effects of thermal metamorphism as much as possible. Our goal was to do a relatively complete characterization of a significant number of these chondrules, including studies of their petrology, cathodoluminescence, mineralogy, major and trace element characteristics, microstructure, and hydrogen isotopic composition. By examining the chondrules in this level of detail, we hoped to understand better the mechanism by which zoning was established, and the nature of the environment in which the chondrules were altered. In addition, we hoped to shed light on what may be the true primary compositions of chondrules.

EXPERIMENTAL

Electron Microprobe

We prepared for this study by making x-ray maps of Semarkona (LL3.0), thin section USNM 1805-7. Methods used to make maps for Na, Mg, Al, S, and Fe on the JEOL 8900 electron microprobe at the U. S. Geological Survey, Reston,

Virginia, USA are outlined in Grossman *et al.* (2000). An area of ~80 mm² of Semarkona was covered. Statistics on the occurrence of zoned chondrules were prepared by visual inspection of the x-ray maps.

Most of the chondrules selected for detailed study were chosen from those found in the x-ray maps of Semarkona thin section USNM 1805-7. Zoning of Na in the mesostases of chondrules 1-2b, 3-3a, 7-2, 7-24 and 7-30 was easily visible in the Na-Kα maps (Fig. 1). An unusual, high-Na, low-FeO chondrule, 7-5, was also selected for study from these x-ray maps. We thought that this might be an example of a type I chondrule in which the process responsible for zoning proceeded to completion. Zoned chondrules 7-31 and 8-20 (found in thin sections USNM 1805-7 and 1805-8, respectively), appeared as low-FeO, barred-olivine chondrules in backscattered electron images. Subsequent x-ray mapping of each of these chondrules revealed the Na-zoning of their mesostasis.

Electron probe microanalyses (EPMA) of mesostasis were made using a focused beam rastered over a 5 × 5 μm area, with 20 nA beam current and 15 kV accelerating voltage; conventional silicate mineral standards were used, and data were reduced using the CITZAF method of Armstrong (1995). Olivine and pyroxene were analyzed with a focused, stationary beam. To minimize the effect of Na loss from mesostasis due to interaction of the electron beam with the sample, Na was determined in the first 10 s after the beam was unblanked. A series of sequential 5 s test analyses of the Na x-ray count rate of several chondrule mesostases showed that susceptibility to Na loss is highly variable, but all analyses done under our conditions should be accurate to within 10%. Each analytical spot was chosen to be as clear of visible crystallites as possible, but in some chondrules the beam inevitably overlapped a small number of these.

In each chondrule, several analytical traverses were made across the mesostasis going from the surface to the interior. In typical chondrules, with <20 vol% mesostasis, the traverses were made by following irregular, sometimes discontinuous channels of mesostasis between the ferromagnesian silicate crystals. The apparent distance of each analytical spot to the chondrule surface was measured from backscattered electron images, defining the surface of the chondrule to be the interface between mafic silicates or mesostasis with any surrounding opaque material, including matrix, rims, and mineral grains. These distances are actually maximum values, as there is a high likelihood that the thin section does not pass through the geometric center of any given chondrule.

Modal abundances of olivine, low-Ca pyroxene, high-Ca pyroxene and mesostasis were measured by image analysis of Mg x-ray maps of each chondrule (Fig. 1). These maps are excellent for this purpose due to the large difference in Mg concentration between the relevant phases. The commercial programs Image Pro Plus and Photoshop were used to do the modal analysis.

Cathodoluminescence

Cathodoluminescence (CL) images of zoned chondrules were obtained using the ELM-3 luminoscope in the Department of Mineral Sciences, National Museum of Natural History, Washington, D.C, USA. A defocused beam at 25 kV accelerating potential and 0.5 mA sample current was used with carbon-coated samples, and CL images were recorded on Kodak Gold 200 print film. For one chondrule, Semarkona 8-20, image processing was done on a scanned CL photograph to obtain an estimate of the relative CL intensity at each point analyzed by EPMA. This was done by measuring the average brightness of the image in the pixels at and immediately surrounding the location of the EPMA spot. While this measurement could be done fairly precisely (estimated ±10%), it is not a quantitative measurement of CL intensity; the latter would require calibration of the film's photographic properties at wavelengths appropriate to the sample. In addition, there are clearly saturation problems in the brightest areas of the image. We consider our method to be only a semiquantitative measurement, but one suitable for examining relationships between CL intensity and other measurements.

Ion Microprobe

Ion probe analyses of trace elements (Rb, Cl, and F) and hydrogen isotopes were carried out on the Department of Terrestrial Magnetism's Cameca 6f ion microprobe. Methods and correction procedures are given by Grossman *et al.* (2000). Analyses were made on four zoned chondrules, plus chondrule 7-5, which has mesostasis that is uniformly high in Na. Four to eight mesostasis areas were measured in each chondrule, including areas as close to the chondrule surface as possible. Because the ion probe has ~20 μm spatial resolution, only this limited number of analyses was possible in each chondrule. For chondrules having abundant tiny crystallites in their mesostasis, the ion probe analyses represent a mixture of these with glass. Accuracy of trace element data is generally better than ±10%.

Transmission Electron Microscopy

Transmission electron microscopy (TEM) was used to look at the mesostasis of one zoned chondrule from Semarkona. The chondrules in the Smithsonian thin sections that were analyzed by EPMA and ion probe methods were not available for TEM work. As described by Grossman *et al.* (2000), demountable, doubly polished petrographic thin sections were prepared from eight small chips of Semarkona (USNM 1805). One of these contained the bleached chondrule analyzed in the earlier study. Another of the sections contained a large zoned chondrule, 1805-7x-1, nearly identical petrographically to chondrule 7-24. This object was studied by optical microscopy, x-ray maps for Na, Ca, Al, Mg, S, and Fe were prepared, and
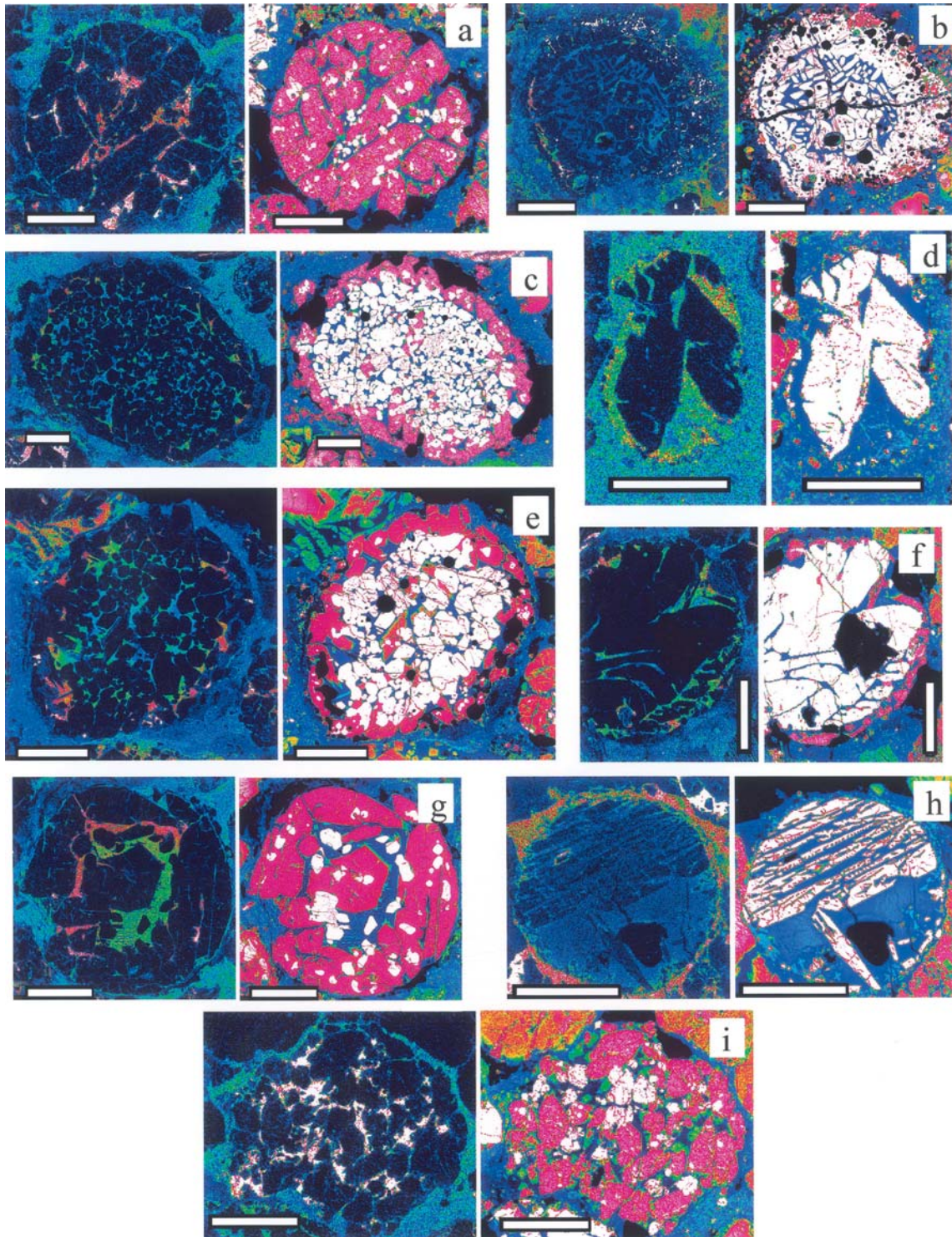
FIG. 1. False-color Na and Mg x-ray maps of Semarkona chondrules. Maps are paired with Na (left) and Mg (right). Colors indicate relative count rates of each element, which from lowest to highest are black-blue-green-yellow-orange-red-pink-white. Within the chondrules in the Na maps, mesostasis ranges from blue to white and mafic silicates are dark-blue to black. Within the chondrules in the Mg maps, olivine appears white, low-Ca pyroxene from red to pink, high-Ca pyroxene green, and mesostasis dark blue. Metal and sulfide are black in all images. (a) Chondrule 7-30 (zoned PP); (b) chondrule 7-31 (zoned BO); (c) chondrule 7-24 (zoned POP); (d) chondrule 3-3a (irregularly zoned PO); (e) chondrule 7x-1 (zoned POP); (f) chondrule 1-2a (zoned POP); (g) chondrule 7-2 (zoned PP); (h) chondrule 8-20 (zoned BO); (i) chondrule 7-5 (unzoned, high-Na, low-FeO POP). All scale bars are 200 μm.

then it was analyzed by TEM. Methods and conditions were described by Grossman *et al.* (2000).

RESULTS

Abundance of Zoned Chondrules in Semarkona

The abundance of zoned chondrules in Semarkona (and other UOCs, based on our unpublished data) is quite large, considering the fact that only a handful of examples have ever been noted in the literature. In the ~80 mm^2 of Semarkona that we x-ray mapped, we identified 62 chondrules and chondrule-fragments as type I (low-FeO, Sears group A) from the Fe x-ray maps. Approximately one-third (22) of these appeared to have some zoning of Na in mesostasis visible in the corresponding Na x-ray maps. Another 5–10 showed uniformly high Na in their mesostasis, but without visible zoning. Among the type II (high-FeO, Sears group B) chondrules, which greatly outnumber type I chondrules (Sears *et al.*, 1992) and which are much richer in alkalis, only a few potentially weakly zoned chondrules were found using the Na maps. Thus, ~15% of Semarkona chondrules are overtly zoned in Na, almost all of which are type I.

Petrology of Zoned Chondrules

Textures–Many of the zoned chondrules selected for our study or noted elsewhere in the literature have classic type I porphyritic textures, as described by Jones and Scott (1989) and Jones (1994), ranging from porphyritic olivine (PO; chondrules 3-3a, plus the one in Matsunami *et al.*, 1993) to porphyritic olivine-pyroxene (POP; chondrules 7-24, 1-2b, 7x-1) to porphyritic pyroxene (PP; chondrules 7-2 and 7-30). Indeed, these chondrules could have been used to draft Fig. 4 in the paper by Scott and Taylor (1983), in which this textural sequence was first described. The other zoned chondrules have typical barred-olivine (BO) textures. These textures can be seen clearly in Mg x-ray maps (Fig. 1) which highlight the difference between olivine, pyroxene and glass. The zoning of Na in the chondrule mesostases can be seen in the Na x-ray maps in Fig. 1. As chondrules were not selected for study on the basis of texture, we assume that this range of textures is typical of zoned chondrules in Semarkona.

The mesostasis of the zoned chondrules in Semarkona ranges from what appears to be clear glass (optically and in backscattered electron) to turbid material rich in pyroxene crystallites; mesostasis within each individual chondrule is more-or-less texturally homogeneous. Small crystals of high-Ca pyroxene, ranging from euhedral to dendritic, occur as isolated grains in the mesostasis or overgrowing large, low-Ca pyroxene crystals. Because low-Ca pyroxene tends to form a shell around the outside of type I POP and PP chondrules, the overgrowths of high-Ca pyroxene may also be more abundant towards the chondrule margins.

Large beads of opaque minerals, mostly kamacite, occur in several zoned chondrules, and tend to be concentrated toward the outer margin and on the rim (abundant in 7-24, 7-31 and 7x-1). Large, "dusty" olivines, rich in finely disseminated Fe-metal occur in the same chondrules (7-24 and 7x-1). Kamacite grains show complex alteration features where they are in contact with the chondrule surfaces, typical of such phases in Semarkona (*e.g.*, Taylor *et al.*, 1981; Hutchison *et al.*, 1987; Alexander *et al.*, 1989; Krot *et al.*, 1997b).

Mineralogy and Zoning Profiles–The mafic mineral chemistry of the zoned chondrules in Semarkona is unremarkable, and very typical of type I chondrules (Table 1). Olivine contains no more FeO than Fa$_{2.5}$ except in chondrule 7-5 (Fa$_4$), which is the one that has uniformly high Na in its mesostasis. The two zoned chondrules dominated by pyroxene, 7-2 and 7-30, contain olivine with >2× as much FeO as do the olivine-rich chondrules, consistent with data of Jones and Scott (1989) and Jones (1994). Based on their mineral and mesostasis compositions (see below) these chondrules belong to Sears' group A2, whereas the olivine-rich ones are group A1 (see Sears *et al.*, 1996). The small crystals of pyroxene in the mesostasis are mostly aluminous diopside in composition, except for those in chondrule 1-2b which are pigeonite.

Microprobe analyses of mesostasis compositions for the zoned chondrules are consistent with features observed in the Na x-ray maps (see Table 2 for summary data and Fig. 2 for plots of individual analyses *vs.* distance from the chondrule surface). Significant decreases in Na content going from surface to interior are observed in all six concentrically zoned chondrules that were probed. In these chondrules, the Na content drops to a constant value in the chondrule core (Fig. 2a). The core concentrations in mesostasis vary from chondrule to chondrule, ranging from <0.5 wt% Na$_2$O in samples 7-31 and 8-20 (the two BO chondrules), up to >3 wt% in 7-2 and 7-30 (the two pyroxene-rich chondrules), with POP chondrules in between. These core values are reached between 75 and 200 μm below the surface of each chondrule. For comparison, the PO Matsunami *et al.* (1993) chondrule reached a constant core Na$_2$O value of ~0.7 wt%, ~300 μm below its surface. Na concentrations in the most enriched, outer parts of the chondrule mesostases are also related to chondrule texture. Maximum values of ~8 wt%, 5–6 wt%, and 1.5–3.5 wt% Na$_2$O occur near the edges of the PP, POP, and BO zoned chondrules, respectively (Fig. 2a).

Potassium closely follows Na in its distribution in zoned chondrules (Table 2), although the data are much less precise in some of the analyses due to poor counting statistics. The Matsunami *et al.* (1993) chondrule also shows K enrichment in mesostasis near its periphery (D. W. G. Sears, pers. comm., 2000, based on a different section through the chondrule; Lyon *et al.*, 1999; Sears *et al.*, 1999), with concentrations of 0.12 wt% K$_2$O in the portion of the chondrule with 2.6 wt% Na$_2$O (note that this unpublished Na value is higher than reported in the original paper, presumably because the zoning profiles are not identical in every part of the chondrule).

Grossman *et al.*

TABLE 1. Compositions of mafic minerals in Semarkona chondrules.

Name	Texture*	N	Na₂O (wt%)	MgO (wt%)	Al₂O₃ (wt%)	SiO₂ (wt%)	P₂O₅ (wt%)	CaO (wt%)	TiO₂ (wt%)	Cr₂O₃ (wt%)	MnO (wt%)	FeO (wt%)	Total (wt%)	ffm† (mol%)
Olivine														
8-20	BO/z	4	<0.02	57.0	0.38	41.8	<0.02	0.55	0.09	0.18	<0.02	1.00	101.0	1.0
7-31	BO/z	5	<0.02	56.7	0.20	42.7	0.04	0.43	0.07	0.17	0.03	0.81	101.2	0.8
Mats‡	PO/z	10	–	55.7	0.25	42.5	–	0.40	0.06	0.15	0.03	0.39	99.5	0.4
3-3a	PO/iz	4	<0.02	57.6	0.18	42.3	<0.02	0.33	0.07	0.26	0.05	0.96	101.8	0.9
1-2b	POP/z	4	<0.02	56.6	0.16	42.6	0.02	0.29	0.03	0.22	0.04	1.36	101.2	1.3
7-24	POP/z	6	<0.02	56.6	0.12	42.8	<0.02	0.30	0.03	0.30	0.12	1.03	101.3	1.0
7-2	PP/z	3	<0.02	55.4	0.03	42.7	<0.02	0.13	0.01	0.42	0.21	2.57	101.4	2.5
7-30	PP/z	3	<0.02	54.6	0.03	42.6	<0.02	0.09	<0.02	0.51	0.34	2.71	100.9	2.7
7-5	POP	2	<0.02	54.9	0.04	40.3	<0.02	0.12	<0.02	0.64	0.69	4.28	101.0	4.2
Low-Ca pyroxene														
1-2b	POP/z	2	<0.02	37.7	1.42	58.8	0.05	0.45	0.19	0.86	0.23	1.41	101.1	2.0
7-24	POP/z	4	<0.02	38.9	1.01	59.2	<0.02	0.40	0.17	0.59	0.17	1.06	101.5	1.5
7-2	PP/z	5	<0.02	38.2	0.34	59.4	<0.02	0.25	0.15	0.47	0.19	1.63	100.7	2.3
7-30	PP/z	1	<0.02	38.7	0.31	59.9	0.06	0.14	0.21	0.46	0.23	1.68	101.7	2.4
7-5	POP	1	<0.02	39.3	0.46	57.4	<0.02	0.29	0.05	0.74	0.50	2.12	100.9	2.9
High-Ca pyroxene														
8-20	BO/z	2	0.09	13.5	18.3	45.9	<0.02	21.6	1.23	0.80	0.11	0.57	102.2	2.3
7-31	BO/z	2	0.32	11.2	17.6	47.7	0.05	21.9	1.68	0.61	0.08	0.85	101.9	4.1
Mats‡	PO/z	5	0.73	13.6	12.0	51.9	–	17.7	1.30	0.67	0.39	0.69	99.0	2.8
1-2b	POP/z	1	0.06	26.5	5.47	54.3	0.04	11.1	1.02	1.62	0.42	1.08	101.5	2.2
7-24	POP/z	3	0.05	18.4	8.59	50.6	<0.02	20.1	1.31	1.39	0.46	0.55	101.4	1.7
7-2	PP/z	3	0.17	15.2	9.34	48.7	<0.02	21.1	0.95	2.95	1.05	1.61	101.0	5.6
7-30	PP/z	3	0.18	17.4	7.35	50.4	0.03	19.9	1.11	2.20	1.30	1.23	101.0	3.8
7-5	POP	1	0.28	19.7	3.89	49.9	0.03	16.5	0.79	1.86	1.04	1.77	95.8	4.8

*Abbreviations: BO = barred olivine; POP = porphyritic olivine-pyroxene; PP = porphyritic pyroxene; z = zoned; iz = irregularly zoned.
†Fe/(Fe + Mg).
‡Data from chondrule reported in Matsunami *et al.* (1993).

Calcium is zoned oppositely to Na in all studied chondrules, with the outermost areas of mesostasis being depleted in Ca relative to that in the chondrule core (Fig. 2b). The magnitude of Ca zoning is smaller than that of alkalis inasmuch as concentrations in mesostasis only vary by a few tens of percent (relative) between cores and outer zones.

Zoning profiles of all other elements in mesostasis measured by EPMA are more complicated, and in some cases less well-defined than those of alkalis and Ca. Aluminum (Fig. 2c) follows Na in two chondrules (one BO and one POP), and is zoned oppositely to Na in three (strongly in one BO and weakly in the two PP chondrules) as well as in the Matsunami *et al.* (1993) PO chondrule. Chondrule 1-2b shows a well-defined Al peak in a zone ~25 μm below its surface, and a second, smaller peak in its core. Silicon is generally anticorrelated with Al (Fig. 2d), and thus is depleted in mesostasis at the margins of some chondrules, and enriched near the surfaces of others. In the two BO chondrules, Mn is relatively low and imprecisely determined in mesostasis (Fig. 2e); Mn probably increases toward the surface of 8-20, but is scattered <0.1 wt% in all points in 7-31. In the POP chondrules 1-2b and 7-24, Mn gradually rises from a core value of ~0.2 wt% to a peak of ~0.6 wt% 50 μm below the surface, before falling back to core

levels in mesostasis just below the surface. Of the two PP chondrules, which both have high core MnO contents of ~1 wt%, one is unzoned in MnO and the other shows an MnO depletion near its surface. Chromium (Fig. 2f) and Ti (Fig 2g) are zoned oppositely to Na in all olivine-rich chondrules, including the one from Matsunami *et al.* (1993) (Table 2), but these elements are scattered and apparently unzoned in the two PP chondrules. Oxidized Fe (Fig. 2h) shows irregular enrichments in mesostasis near the margins of several olivine-rich chondrules, and is distinctly enriched ~75 μm below the surface of BO chondrule 7-31. Finally, Mg (not illustrated) is essentially unzoned in mesostases in all of the chondrules except PP chondrule 7-2, in which MgO rises from ~2 wt% near the edge to ~6 wt% in the core.

Mesostasis in POP chondrule 7x-1 was only analyzed in a few points by TEM using energy-dispersive x-ray spectrometry (EDS) (Table 2). These data, although lower in quality and in scope than our EPMA traverses, show that 7x-1 probably shares many properties with the chondrule that it most closely resembles texturally, 7-24. Mesostasis near the edge is high in Na and Al, and low in Ca, Cr, Mn, and Ti. The difference in Ca between core and edge appears to be the most extreme of any measured chondrule, although the statistics of small numbers and differences in analytical methods may play a role here.
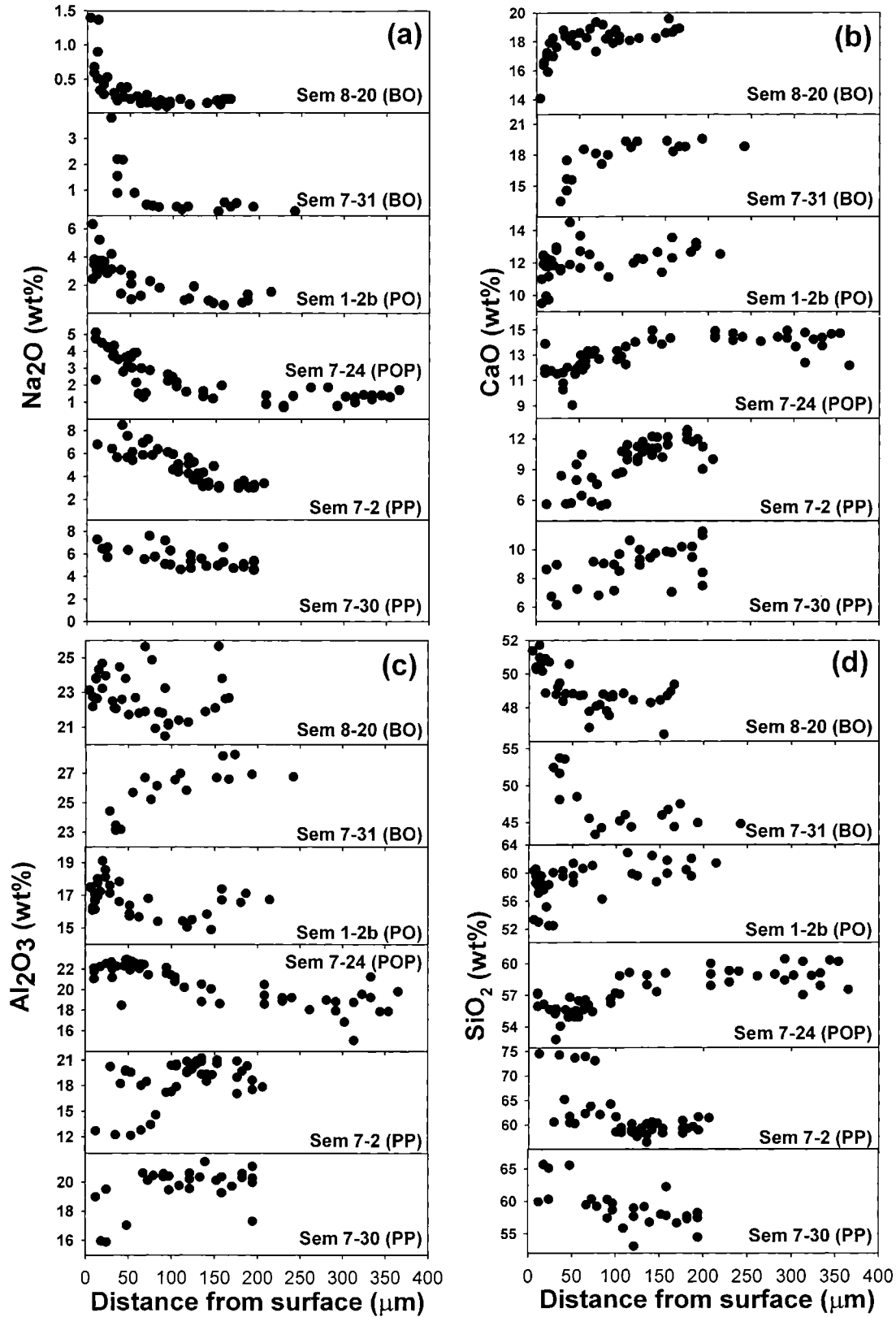
FIG. 2. Zoning profiles in mesostasis of Na (a), Ca (b), Al (c), and Si (d) across concentrically zoned, low-FeO chondrules from Semarkona. Chondrules have been arranged from olivine-rich at the top to pyroxene-rich at the bottom of each part of the figure. Distances are measured to the nearest interface between chondrule silicates and surrounding matrix or rims. In each case, the rightmost point is near the chondrule center. Each point represents a single electron microprobe analysis. *Figure 2 is continued on the next page.*
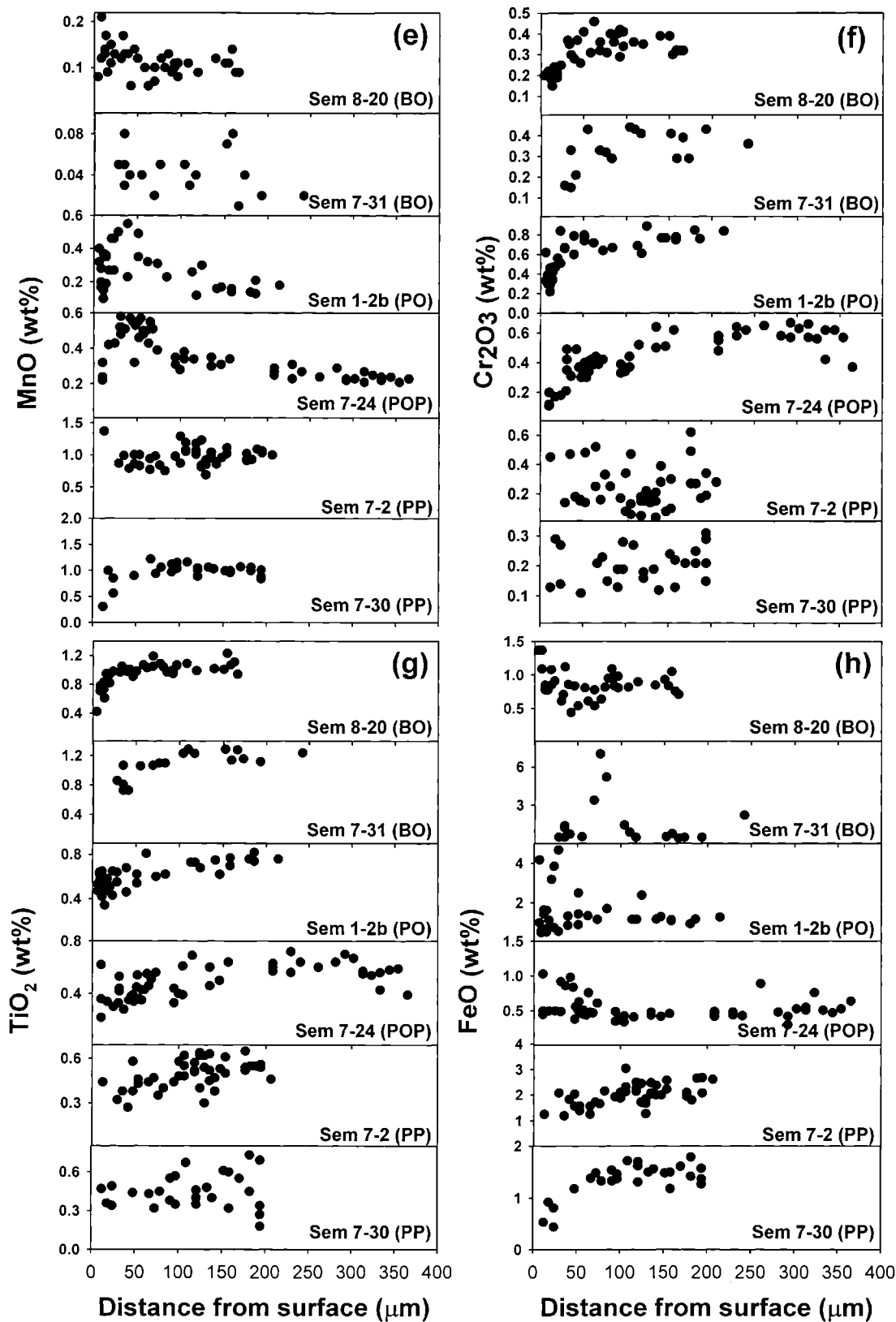
FIG. 2. *Continued.* Zoning profiles in mesostasis of Mn (e), Cr (f), Ti (g), and Fe (h) across concentrically zoned, low-FeO chondrules from Semarkona. Chondrules have been arranged from olivine-rich at the top to pyroxene-rich at the bottom of each part of the figure. Distances are measured to the nearest interface between chondrule silicates and surrounding matrix or rims. In each case, the rightmost point is near the chondrule center. Each point represents a single electron microprobe analysis.

TABLE 2. Compositions of mesostasis in Semarkona chondrules.*

Name	N	Distance (μm)	Na₂O (wt%)	MgO (wt%)	Al₂O₃ (wt%)	SiO₂ (wt%)	P₂O₅ (wt%)	Cl (wt%)	K₂O (wt%)	CaO (wt%)	TiO₂ (wt%)	Cr₂O₃ (wt%)	MnO (wt%)	FeO (wt%)	Total (wt%)
8-20 (BO/z)															
edge	1	4	1.40	10.24	23.14	51.39	0.02	0.00	0.06	14.10	0.42	0.20	0.08	1.37	102.42
↓	5	8–13	0.81	7.93	23.04	50.79	0.00	0.04	0.05	16.62	0.73	0.19	0.15	0.98	101.35
	12	15–58	0.31	8.14	23.18	49.46	0.01	0.02	0.03	18.14	0.97	0.30	0.12	0.79	101.46
core	18	62–166	0.16	9.84	22.47	48.36	0.00	0.01	0.03	18.63	1.05	0.36	0.10	0.84	101.85
7-31 (BO/z)															
edge	1	28	3.79	4.70	24.43	52.47	0.03	0.00	0.18	13.52	0.86	0.16	0.05	0.49	100.68
↓	3	35–41	1.97	4.20	23.26	52.99	0.06	0.09	0.06	15.88	0.84	0.23	0.06	0.87	100.78
core	14	55–242	0.36	4.36	26.74	45.26	0.01	0.06	0.03	18.71	1.19	0.37	0.03	1.95	99.60
Matsunami chondrule† (PO/z)															
edge		0–75	2.6	4.7	18.2	59.7	–	–	0.12	14.1	0.83	0.23	0.16	0.9	101.6
core		200–400	0.7	7.0	22.0	52.0	–	–	<0.02	16.0	>1.2	>0.6	0.10	0.4	
3-3a (PO/iz)															
High-Na	4	7–31	3.81	5.47	15.37	60.27	0.01	–	0.28	12.23	0.73	0.35	0.21	0.60	99.33
Intermed.	7	6–97	2.69	5.74	16.94	59.26	0.01	–	0.22	12.62	0.85	0.51	0.23	0.62	99.70
Low-Na	3	26–43	1.14	7.64	15.75	60.31	0.02	–	0.12	13.42	0.77	0.58	0.34	0.61	100.70
1-2b (POP/z)															
edge	1	6	6.32	4.89	17.52	60.33	0.00	–	0.39	9.52	0.53	0.33	0.32	0.98	101.14
	12	8–20	3.62	6.73	17.02	58.11	0.03	–	0.21	11.65	0.54	0.38	0.26	1.59	100.14
	8	23–51	2.40	5.97	17.09	57.86	0.01	–	0.15	12.72	0.57	0.71	0.42	2.03	99.94
↓	7	62–141	1.45	6.25	15.67	60.39	0.01	–	0.11	12.08	0.70	0.71	0.24	1.43	99.05
core	6	146–186	0.82	7.16	16.64	60.41	0.03	–	0.05	12.69	0.73	0.78	0.16	1.13	100.59
7-24 (POP/z)															
edge	3	10–17	4.78	4.67	22.04	56.44	0.00	–	0.24	11.75	0.31	0.13	0.29	0.67	101.32
	6	24–36	3.89	5.28	21.99	54.80	0.01	–	0.22	11.31	0.38	0.33	0.51	1.20	99.90
	9	42–57	3.33	5.65	22.14	55.55	0.00	–	0.18	11.80	0.40	0.37	0.50	0.60	100.51
↓	15	60–156	1.96	4.95	21.10	57.24	0.01	–	0.12	13.45	0.50	0.45	0.38	0.46	100.62
core	16	208–354	1.12	5.42	18.70	59.07	0.01	–	0.06	14.31	0.60	0.58	0.25	0.49	100.60
7x-1 (POP/z)‡															
edge	2	<100	3.6	2.8	21.1	57.0	–	–	0.3	12.8	0.7	0.3	0.5	1.0	≡100
core	1	>100	2.2	3.6	14.6	52.1	–	–	0.3	22.3	1.0	0.8	1.1	2.0	≡100
7-2 (PP/z)															
edge	14	12–94	6.47	2.57	16.38	66.47	0.01	0.01	0.56	7.22	0.41	0.27	0.93	1.66	102.96
	11	100–124	4.81	3.36	19.74	59.06	0.02	0.01	0.28	10.53	0.54	0.19	1.06	2.21	101.80
↓	11	129–153	3.70	3.81	20.22	59.03	0.00	0.01	0.25	11.24	0.50	0.18	0.93	2.06	101.94
core	8	176–206	3.22	4.75	18.88	59.93	0.01	0.01	0.25	11.39	0.55	0.33	1.00	2.24	102.54
7-30 (PP/z)															
edge															
	2	12–18	6.87	3.58	17.48	62.79	0.02	–	0.54	7.69	0.41	0.21	0.66	0.73	100.95
	3	24–48	6.20	3.15	17.49	63.65	0.01	–	0.55	7.46	0.42	0.17	0.77	0.81	100.68
↓	12	67–133	5.72	3.69	20.22	58.32	0.02	–	0.37	8.97	0.45	0.20	1.06	1.48	100.47
core	10	139–194	4.96	4.71	20.12	56.88	0.02	–	0.31	9.74	0.48	0.22	0.97	1.67	100.09
7-5 (POP)															
Meso	1	–	9.37	2.25	20.38	59.03	0.00	0.00	0.68	3.42	0.53	0.05	0.70	1.48	97.88

*For radially zoned chondrules, all analyses have been grouped and averaged according to distance from the chondrule surface. For chondrule 3-3a, which shows irregular zoning, three subsets of similar analyses have been averaged to show the range of alkali contents. Chondrules have been grouped according to texture. See Table 1 for explanation of abbreviations.

†Edge data from D. W. G. Sears (pers. comm., 2000) based on the section reported in Lyon *et al.* (1999) and Sears *et al.* (1999). Core data from Matsunami *et al.* (1993), except K₂O, TiO₂ and Cr₂O₃ extrapolated from D. W. G. Sears (pers. comm., 2000).

‡Measured by TEM using energy-dispersive x-ray spectrometry.

Chondrule 3-3a (PO) has irregularly zoned mesostasis in that Na enrichments occur both near the chondrule surface and in the chondrule interior near the mesostasis–olivine interfaces. In common with all of the symmetrically zoned chondrules, K correlates with Na, and Ca anticorrelates with Na in 3-3a mesostasis analyses. As in the other four measured olivine-rich zoned chondrules, Cr and Ti are depleted in regions where Na is enriched in 3-3a. However, Mn is depleted in Na-rich areas, a property shared only with PP chondrule 7-30. Mg also anticorrelates with Na in 3-3a, similar only to PP chondrule 7-2. Aluminum, Si and Fe do not correlate with Na, although Al and Si are anticorrelated.

Cathodoluminescence–CL images were obtained for six of the seven zoned chondrules studied by EPMA (all except for PP chondrule 7-2). The Matsunami *et al.* (1993) chondrule was noteworthy for its CL zoning, and had yellow-luminescent mesostasis that was brightest near the surface. This same effect was observed in BO chondrules 7-31 and 8-20, and POP chondrules 7-24 and 1-2b (1-2b showed the brightest CL near its edge of any of the chondrules). PP chondrule 7-30 shows uniform dull yellow CL, with one patch of brighter yellow CL near one side. Irregularly zoned chondrule 3-3a has nonluminescent mesostasis. As expected, olivine in many of the chondrules shows red CL, a trait typical of forsteritic olivine in UOCs. A direct comparison of the CL and alkali zoning features of chondrules 7-24 and 8-20 (Fig. 3) shows that Na enrichment and bright yellow CL both occur preferentially in the outer zone of the chondrules, but the correspondence is
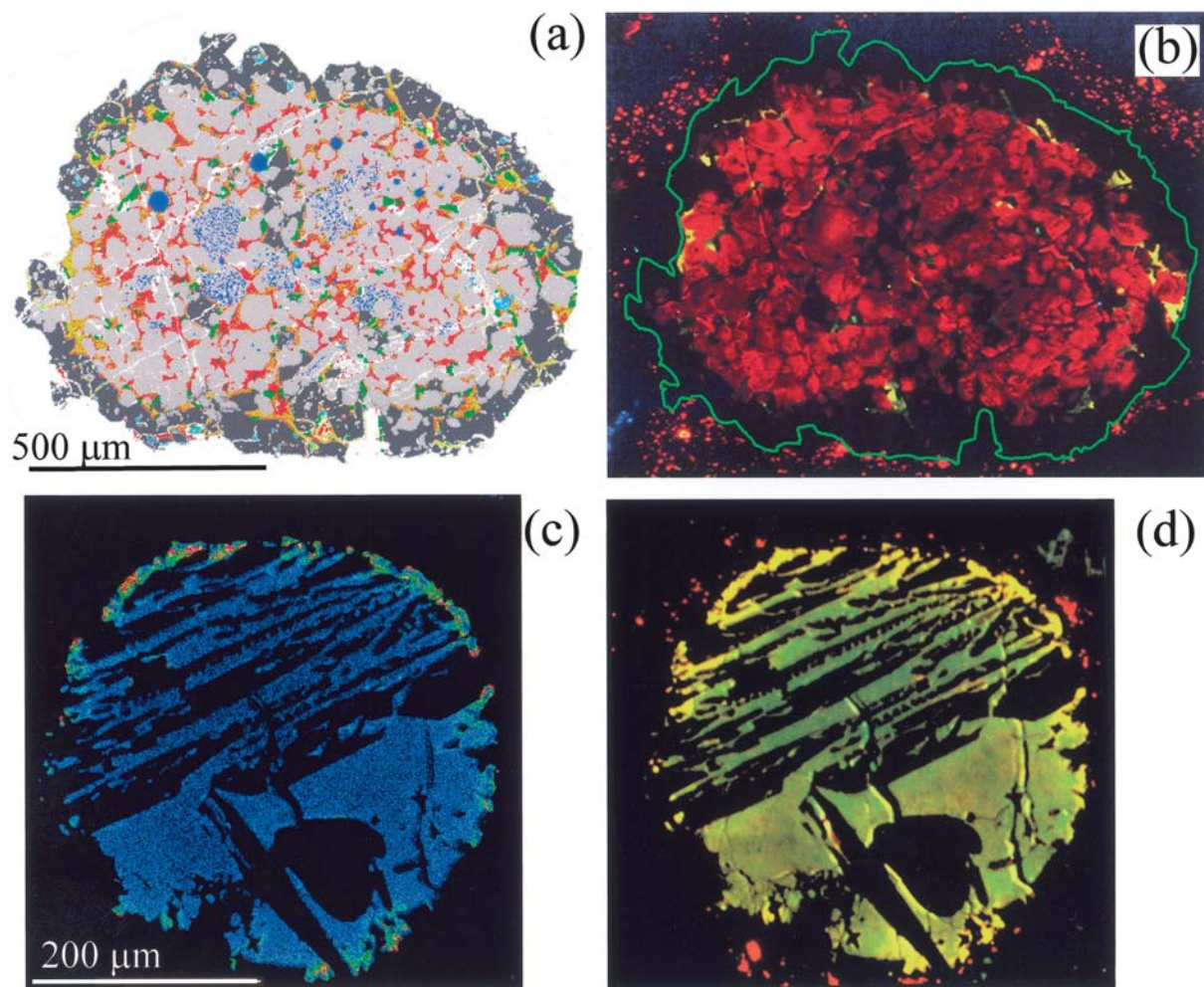

FIG. 3. (a) Schematic representation of the mineralogy of chondrule 7-24 (zoned POP) based on Na, Ca, Fe, Mg, and Al x-ray maps. Mesostasis ranges from high-alkali (yellow) to low alkali (red) content. Low-Ca pyroxene appears dark gray, olivine light gray, high-Ca pyroxene green, and metal/sulfide blue. White lines are cracks. (b) CL image of chondrule 7-24, showing characteristic red CL of olivine and yellow CL of mesostasis; pyroxene is nonluminescent. Alkali-rich mesostasis—compare (a)—toward the chondrule edge is brighter yellow than in the interior. The green line denotes the boundary of the chondrule with its metal/sulfide-rich rim. (c) Sodium x-ray map of BO chondrule 8-20, where surrounding material (Na-bearing matrix) has been digitally masked out to allow easy recognition of zoning trends within the mesostasis. Color-scheme is as in Fig. 1. (d) CL image of chondrule 8-20 showing the strong zoning in mesostasis. Most black parts of the chondrule are olivine, except the tiny "x"-shaped crystals in the yellow mesostasis and just inside the chondrule surface which are aluminous diopside.

not perfect. In sample 7-24, bright yellow CL is associated with the pyroxene-rich outer shell of the chondrule, and not all areas of mesostasis having the brightest CL are especially high in Na (e.g., the bright yellow patch near the bottom center of Fig. 3b). In chondrule 8-20, the correspondence between bright CL and Na is somewhat better (Fig. 3c,d). Our semiquantitative estimate of CL intensity does correlate with Na (Fig. 4), and much of the observed scatter in the CL-Na trend can be related to position in the chondrule: most of the points forming what looks like a lower-slope array come from the more olivine-rich, upper half of the chondrule as shown in Fig. 3c,d, whereas the higher-slope trend derives from the more glass-rich area. (Data plotting near 100% CL intensity in Fig. 4 came from areas of the CL image that were nearly fully saturated yellow, and thus differences among these points cannot be resolved.)

Ion Probe Data—We analyzed four zoned chondrules (the four porphyritic ones with concentric mesostasis zoning) plus the alkali-rich POP chondrule, 7-5, by ion microprobe for major and trace elements and hydrogen isotopes (Table 3). Our main goal was to understand better the behavior of volatile elements, so our data include the moderately volatile alkalis, Na, K, and Rb, and halogens, F and Cl, as well as H which we report as H_2O. Data for major element oxides in chondrule mesostases agree well with EPMA data listed in Table 2. The ranges of Al_2O_3, Na_2O, and K_2O measured by EPMA are summarized in Table 3 for comparison with ion probe results; other major element data by ion probe are not shown, and will not be used for our discussion.

Although ion probe spots were carefully located on each sample, direct presentation of zoning profiles that we measured by ion probe are not particularly helpful. We measured only 5–8 spots in each chondrule, and because of the large (20 μm) spot size, it was impossible to analyze small areas of mesostasis and mesostasis immediately adjacent to the chondrule surface. Analyses were also scattered across each chondrule, rather than forming any kind of orderly traverses from core to rim. We have established by EPMA methods (above) that these chondrules are generally, but not perfectly, concentrically zoned. Some of the scatter in Fig. 2 can be accounted for by the presence of somewhat different zoning profiles along different core–rim traverses. Because of these factors, and because Na is well determined by both EPMA and ion probe, we chose to present the ion probe data as scatter plots of elemental abundances (relative to Al) vs. that of Na (Figs. 5 and 6). In these diagrams, points with low and high Na/Al ratios should be considered as representative of the chondrule cores and outer zones, respectively.

The abundances of four moderately volatile trace elements, K, Rb, F, and Cl, correlate well with that of Na in all four zoned chondrules (Fig. 5). With only one exception, every point analyzed in these chondrules shows element/Na ratios for K, Rb, F, and Cl that are lower than the ratio in either CI chondrites or the host, LL-chondrite group (data from Wasson and Kallemeyn, 1988). Potassium and Na show the simplest
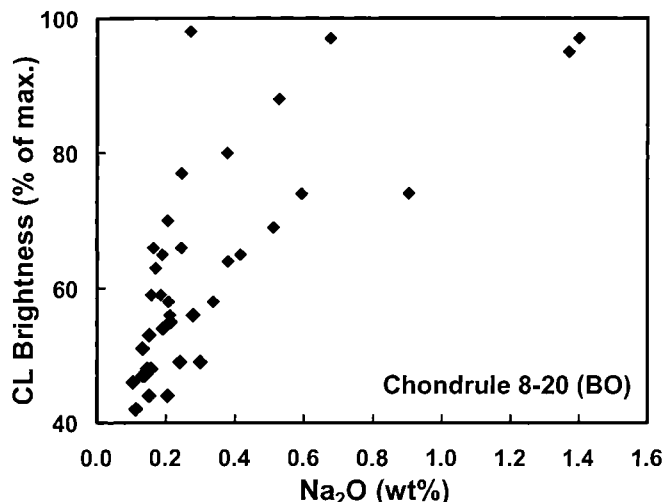

FIG. 4. Relative intensity of yellow CL vs. Na_2O content in BO chondrule 8-20 (see also Fig. 3). CL intensity was measured by digital image processing, and represents brightness relative to the most intense yellow part of the chondrule. Sodium was measured by EPMA. The correlation between CL and Na is generally strong, with different parts of the chondrule giving rise to what appear to be higher and lower slope trends.

relationship (Fig. 5a), with the PO and POP chondrules plotting at lower abundances of both elements as well as lower K/Na ratios than the two PP chondrules. Regression lines through the analyses in individual chondrules (dashed lines) extrapolate to near or slightly above the origin, showing that K/Na ratios are either constant or decrease from core to rim. Mesostasis in the unzoned, Na-rich chondrule, 7-5, has higher abundances of Na and K than any points in the zoned chondrules, and plots near extrapolations of most of the zoned-chondrule regression lines.

Plots of Rb vs. Na abundances in mesostasis of zoned chondrules (Fig. 5b) resemble K vs. Na plots in that Rb and Na are extremely well correlated in each chondrule. No significant difference in Rb abundance is seen between POP and PP chondrules. All areas of the chondrules, cores and surfaces, appear to be more depleted in Rb relative to Na than they are in K, and Rb/Na ratios change (rise) dramatically going from core to surface in most chondrules. Rb/Al ratios are <0.1 × (CI or LL) in the cores of all the chondrules, and these ratios rise to about 0.3–0.5 in the most Na-rich mesostasis areas, where the Na/Al ratio is approximately chondritic, near the surfaces. Again, chondrule 7-5 plots almost exactly on extrapolations of regression lines through data for zoned chondrules to higher alkali content.

Data for the halogens in mesostasis are more scattered than those of alkali elements, but all of the zoned chondrules show enrichment of both F and Cl in high-Na areas near the chondrule surfaces (Fig. 5c,d). As with Rb/Al, chondrule cores have very low F/Al and Cl/Al ratios. Halogen/Na ratios rise in the outer parts of the chondrules to (0.5–1) × LL-group levels from values <0.1 in the cores (probably near blank levels). Chondrule 7-5 mesostasis has a fairly low F/Al ratio, and only lies near the

TABLE 3. Ion microprobe data for Semarkona chondrule mesostases.*

	Al$_2$O$_3$ (wt%)	Na$_2$O (wt%)	K$_2$O (wt%)	Rb (ppm)	F (ppm)	Cl (ppm)	H$_2$O (ppm)	δD (‰)
1-2b (POP/z)	(15–19)	(0.6–6.3)	(0.03–0.39)					
p36	19.6	7.01	0.39	5.0	202	412	3280	843 ± 19
p40	17.9	5.68	0.30	6.2	807	2690	5470	645 ± 20
p4	18.4	4.09	0.18	3.5	271	510	2530	447 ± 18
p34	17.8	3.22	0.17	0.24	32	161	843	753 ± 77
p41	20.2	3.20	0.11	1.34	60	108	9800	47 ± 11
p21	18.5	2.92	0.15	0.48	190	195	920	1690 ± 73
p13	14.6	1.39	0.088	0.00	44	24	840	710 ± 64
7-24 (POP/z)	(15–23)	(0.7–5.1)	(0.05–0.28)					
p8	23.3	4.36	0.096	3.3	n.d.	148	1390	1960 ± 43
p6	19.3	4.08	0.085	3.3	n.d.	26	1770	2340 ± 300
p4	23.8	3.94	0.068	2.1	n.d.	63	515	1270 ± 150
p2	19.5	1.39	0.026	0.84	n.d.	6.5	395	806 ± 120
p1	24.1	1.36	0.030	1.02	n.d.	4.6	146	616 ± 66
p3	22.5	1.31	0.029	1.17	n.d.	4.0	299	1050 ± 90
p5	21.0	1.26	0.021	0.87	n.d.	13	337	454 ± 24
p7	26.0	1.05	0.041	1.11	n.d.	17	135	315 ± 42
7-2 (PP/z)	(12–21)	(3.0–8.5)	(0.17–0.83)					
p6	17.1	7.09	0.40	7.5	144	276	2450	1260 ± 26
p5	11.8	5.02	0.38	7.9	6.2	3.1	1320	1230 ± 48
p4	15.8	3.88	0.22	3.8	46	37	2860	2010 ± 89
p7	20.8	2.82	0.20	0.32	5.0	2.4	236	732 ± 87
p3	16.7	2.76	0.24	0.39	2.9	2.2	212	240 ± 51
7-30 (PP/z)	(16–21)	(4.6–7.6)	(0.25–0.68)					
p29	18.5	7.88	0.44	6.9	431	310	1720	1280 ± 38
p27b	18.6	6.12	0.35	5.3	141	250	1720	–
p27	20.2	5.54	0.35	4.7	13	14	1100	1200 ± 44
p25	13.1	4.47	0.29	4.6	146	353	704	1110 ± 29
p26	19.5	4.39	0.23	1.83	23	15	880	2040 ± 72
p10	–	2.24	–	–	–	–	346	959 ± 49
7-5 (POP)	(19–21)	(7.4–9.4)	(0.6–0.7)					
p1	–	–	–	–	–	–	–	141 ± 14
p2	–	–	–	–	–	–	–	325 ± 18
p4	21.5	12.3	0.83	13.4	128	1100	4050	1120 ± 47
p5	–	–	–	–	–	–	–	707 ± 28
p6	–	–	–	–	–	–	–	785 ± 24

*Numbers shown in parentheses for Al$_2$O$_3$, Na$_2$O and K$_2$O are ranges of all points measured by electron microprobe.
Data are arranged in order of decreasing Na$_2$O contents. See Table 1 for explanation of abbreviations.

extrapolation of one zoned-chondrule trend (7-2). However, 7-5 is quite enriched in Cl, and these data resemble those of K and Rb in lying along extrapolations of most zoning trends.

Data for elemental hydrogen, calculated as H$_2$O, are summarized in Fig. 6. Although we have no direct evidence that water is the actual form of H$_2$O in chondrule mesostasis, we think this is likely, and will discuss the data in these terms. Water contents in the zoned chondrule mesostases are highly variable, ranging from 100 to 200 ppm in the cores of two zoned chondrules to ~1 wt% in one point in chondrule 1-2b. Water content correlates well with Na abundance in three of the chondrules, and it would in all four chondrules if the one very high-water point in 1-2b is ignored (Fig. 6a). δD also spans a wide range among the zoned chondrules and within individual chondrules. Chondrule 7-24 and 7-2 show strong correlations (defined here and below as >95% confidence level) between δD and water content (Fig. 6b), and between δD and Na abundance, with the core of the chondrules having δD = +200–300‰, and mesostasis near the margins having δD = +1700‰ (7-24) to +3000‰ (7-2). Chondrule 7-30 shows a strong correlation between Na abundance and water content, and weak positive δD–water and δD–Na correlations. The relationships for chondrule 7-30 involving δD are mainly destroyed by one anomalously high-D/H measurement, without which these
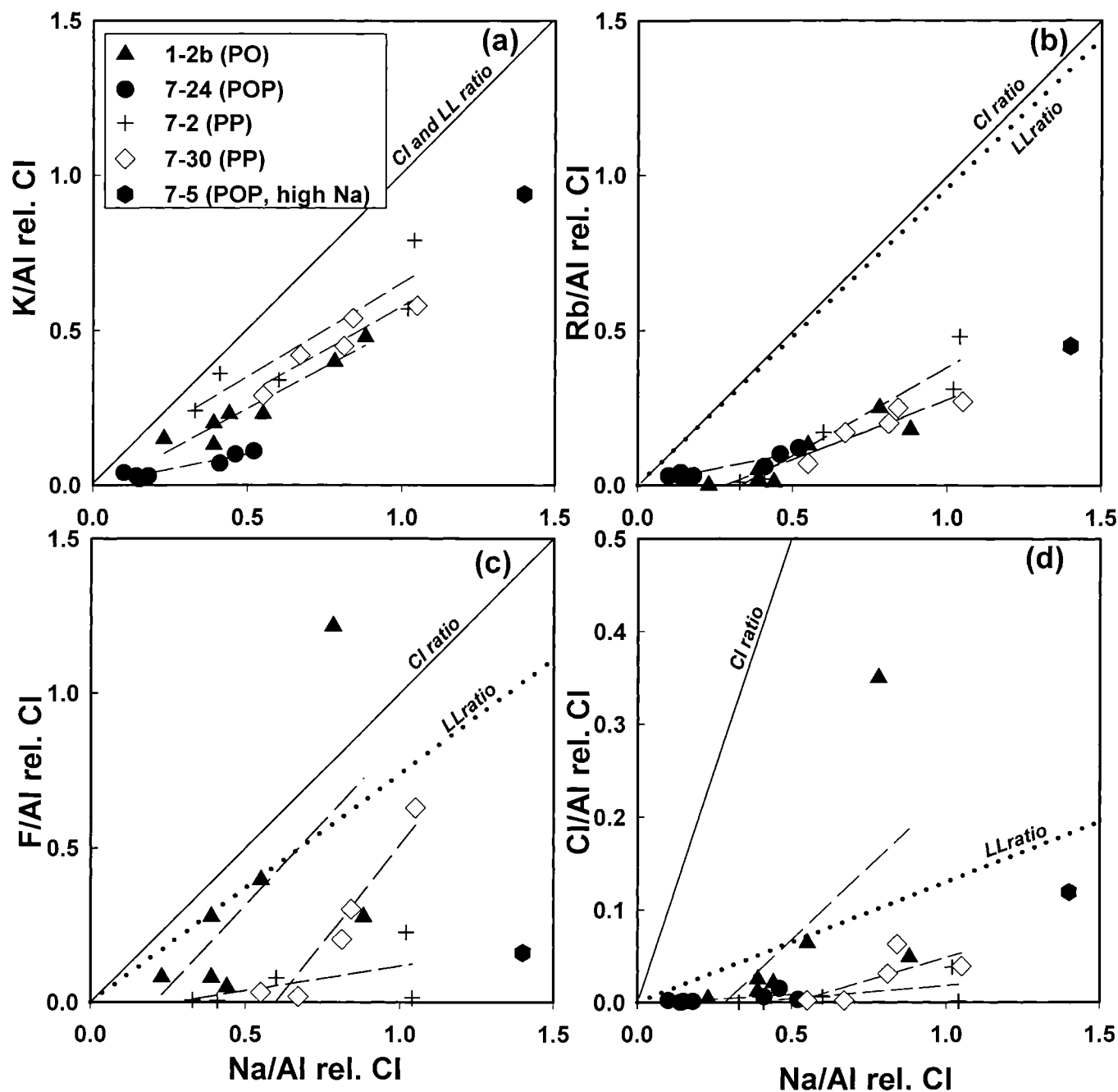
FIG. 5. Ion probe measurement of alkalis and halogens in mesostasis from four zoned chondrules plus Na-rich, FeO-poor chondrule 7-5. (a) K vs. Na; (b) Rb vs. Na; (c) F vs. Na; (d) Cl vs. Na. All data are normalized to Al and to the CI chondrites, with the bulk LL and CI ratios shown for reference (chondrite data from Wasson and Kallemeyn, 1988). Dashed lines show linear regressions through data from each chondrule (except 7-5, which only has a single analysis). Potassium, Rb, Cl, and F are all strongly to fairly well correlated with Na in all chondrules.

correlations would all be strong. Chondrule 1-2b seems to show an anticorrelation between δD and water, even if the anomalously water-rich point ("p41" in Table 3) is ignored.

Transmission Electron Microscope Results–Two areas of Semarkona chondrule 7x-1 were examined by TEM: one was in the olivine-rich central area of the chondrule, the other close to the surface, in the pyroxene-rich outer zone. In both examined areas, the mesostasis appears to be dominated by

glass. In this phase, electron diffraction patterns show broad diffuse rings indicative of amorphous material, and there are no sharp diffraction maxima that might arise due to the formation of crystalline phases during alteration reactions or devitrification. EDS obtained on the TEM show that the core region is much richer in Ca and poorer in Na than the outer region, despite the fact that both are amorphous. Some traces of phyllosilicates were found around glassy areas, but the great
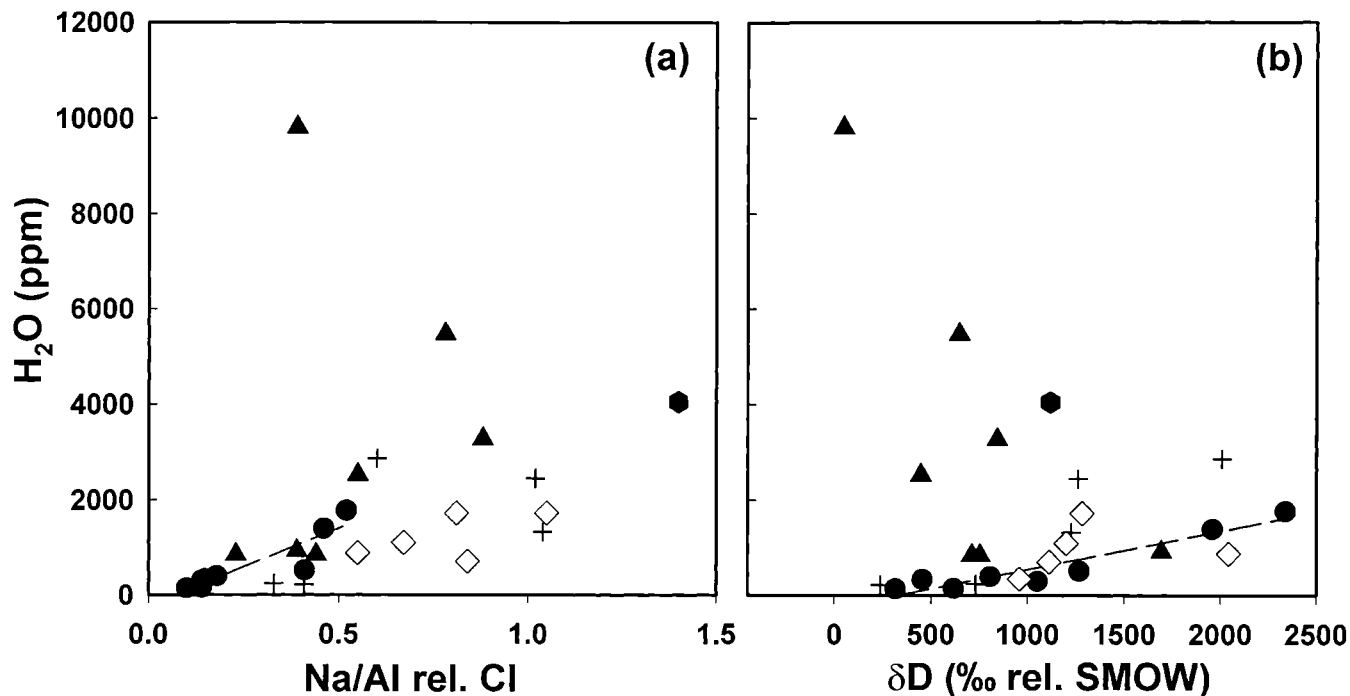
FIG. 6. Ion probe data for H (reported as H_2O), deuterium (reported as δD relative to standard mean ocean water (SMOW)) and Na in mesostasis of four zoned chondrules plus Na-rich, FeO-poor chondrule 7-5. (a) Total H_2O *vs.* Na (normalized as in Fig. 5). (b) Total H_2O *vs.* δD. Significant correlations are present among these variables for all chondrules except 1-2b, the most water-rich sample. A linear regression line is shown for chondrule 7-24, which shows the strongest correlations of any chondrule. Symbols as in Fig. 5.

majority of the mesostasis appears to be free from these phases. In the outer region of the chondrule, this even applies to mesostasis that is immediately adjacent to a large, chemically altered kamacite grain. Sodium enrichment in outer zones is clearly a feature of glass, and not due to the presence of phyllosilicates.

DISCUSSION

The critical observations we have made that must be taken into account when explaining the origin of zoned chondrules in Semarkona are: (1) Assuming chondrule 7x-1 is representative, glass is present in all parts of zoned mesostasis, and secondary alteration products are rare. (2) The moderately volatile elements, including alkalis (Na, K, Rb) and halogens (F, Cl), behave as a group, and are all enriched in the outer areas of mesostasis in all zoned chondrules. (3) The highly volatile element H follows the moderately volatile elements in most zoned chondrules; zones enriched in H also tend to have high D/H ratios. (4) Volatile elements in mesostasis are strongly anticorrelated with Ca. (5) With the exceptions of Fe and Mg, most elements more refractory than the alkalis are also zoned; zoning profiles of these elements are not the same in every chondrule, and there are relationships between chondrule mineralogy and zoning.

Two other key observations are shown schematically in Fig. 7, in which we recalculate the mesostasis compositional trends of two representative chondrules, 8-20 (BO) and 7-24 (POP). (6) The core-to-edge zoning profiles, normalized to their maximum and minimum concentrations, are very similar in shape for many elements. The distance below the chondrule surface at which the concentration is about halfway between the maximum and minimum values, regardless of whether the element is enriched or depleted at the surface, varies only by a small amount, and may not vary at all given the uncertainties in some of the minor element zoning patterns. And, (7) near the position of the mineralogical break between the inner olivine-rich zone and the outer pyroxene-rich zone in POP chondrules like 7-24 (Fig. 7a), zoning profiles for some elements (*e.g.*, Mn and Al) change direction, whereas other elements (*e.g.*, alkalis and Cr) do not.

It is probably impossible to account for all of these observations with a simple model in which zoning originates during a single phase of chondrule history. It is unlikely that enrichment of an element as volatile as H to levels >0.2 wt% H_2O could occur at a temperature anywhere near that at which the chondrule is partially molten, or even as high as the condensation temperatures of the moderately volatile elements (~1000 K for the alkalis under canonical solar-nebula conditions; Wasson, 1985). Volatiles such as water are lost rapidly from chondrule-like melts (*e.g.*, Maharaj and Hewins, 1998), and mark their presence with persistent vesicles in such experimental charges. In unpublished data (L. Grossman, pers. comm., 2000) that was part of the study of Ebel and Grossman
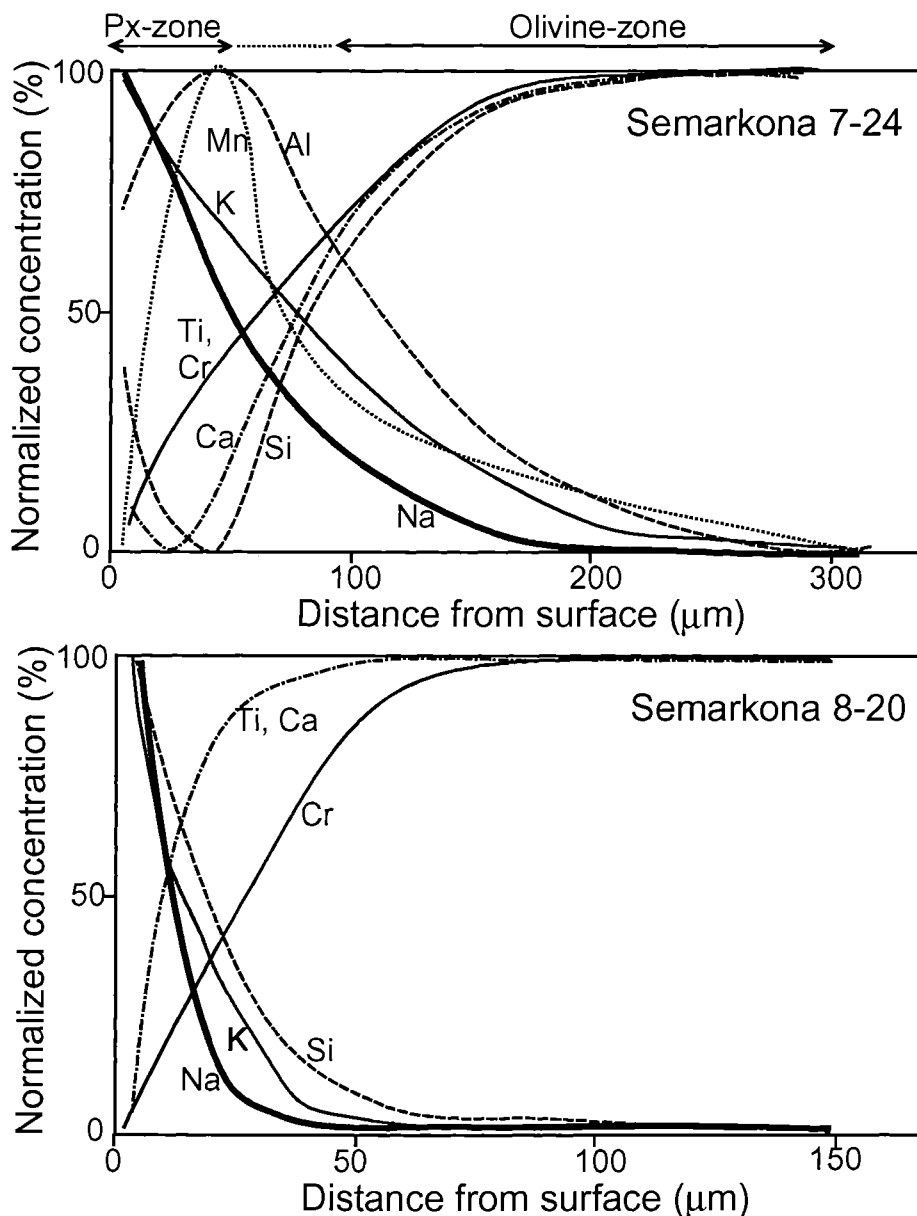
FIG. 7. Normalized zoning patterns in POP chondrule 7-24 and BO chondrule 8-20. In order to compare the shapes of zoning profiles, each element has been normalized to the average core value (either 0 or 100% depending on whether the element is lower or higher in the core), and to the value in the outer zone (100% or 0, again depending on the direction of zoning) either at the extreme outer margin or, in the case of some elements in 7-24, where the element shows its maximum/minimum value. The result of this is a family of curves ranging from 0 to 100%, which were drawn by eye through the point data. Any element not shown is either unzoned, or too poorly determined to present a meaningful curve. Note that the general shapes of the curves in each chondrule, whether increasing or decreasing, are very similar from element to element.

(2000), silicate liquids calculated to form at 1000× dust enrichments and 10^{-3} bar only contained ~10 ppm H_2O at 1460 K. Water does not become an important alteration reactant in the solar nebula or on parent bodies unless the temperature is below ~500 K (e.g., references cited in Bischoff, 1998; Sears and Akridge, 1998). This suggests that zoning of H and, by extension elements that strongly correlate with H, occurred at low temperatures, probably in the parent asteroid where

aqueous processes are known to have occurred. However, the lack of secondary alteration minerals and the preservation of igneous glass in mesostasis rich in volatiles seem more consistent with a high-temperature origin rather than a process like aqueous alteration which might be expected to lead to devitrification and formation of hydrated phases. Ubiquitous zoning of major elements in these chondrules, and the fact that relationships exist between igneous mineralogy and the zoning

profiles of nonvolatile elements also point to a high-temperature origin for some of the zoning effects. Certainly, the change in zoning direction at the pyroxene-olivine boundary in POP chondrules strongly suggests that igneous processes may be at work. Thus it appears that zoning may have been established over a wide range of temperatures and by more than one process. Is it possible to untangle this complicated picture in order to understand the individual processes and environments involved?

On the basis of their data on one Semarkona chondrule, Matsunami *et al.* (1993) evaluated six processes as possible explanations for their observations of mesostasis zoning: fractional crystallization of the original melt, Soret diffusion due to internal temperature gradients, entry of elements during aqueous alteration, melting of inhomogeneous precursor material, recondensation of evaporated material into hot chondrules, and reduction of ferroan material. They rejected low-temperature processes on the basis of a lack of aqueous alteration products, and concluded that the enrichment of the moderately volatile elements Na and Mn in the outer zone of the chondrule was due to the recondensation of these elements, lost during the melting event, onto the surface of the cooling chondrule, with subsequent diffusion into the interior. Matsunami *et al.* (1993) explained the depletion of Ca and Al and enrichment of Si at the chondrule surface by reduction and loss of FeO that may have been present in precursor olivine, resulting in SiO_2 enrichment at a reaction front near the chondrule surface; enhancement of SiO_2 caused depletion of CaO and Al_2O_3 due to mass-balance (dilution) effects. This is essentially a two-step process, one igneous (reduction during melting) and the other probably subsolidus, while the chondrule was cooling.

However, our new data show that the Matsunami *et al.* (1993) chondrule occupies just one part of a spectrum of zoning profiles that occur in low-FeO chondrules in Semarkona. The zoning of alkalis is one property that the Matsunami chondrule has in common with all the chondrules we studied. Similarly, the Matsunami chondrule and all of our zoned chondrules show an inverse correlation between Na and Ca, where Ca is depleted near chondrule surfaces. But, some chondrules that we studied are oppositely zoned in Si, Al and Mn to the Matsunami chondrule, or are not zoned at all in these elements. With these differences in mind, and in light of our new data on other elements, especially H, which seem to demand further assessment of low-temperature processes, a reevaluation of the conclusions of Matsunami *et al.* (1993) is in order. Therefore, we will proceed to reexamine chemical processes that might have resulted in elemental zoning during the various episodes of chondrule history.

High-Temperature Processes

High-temperature processes that might result in chondrule zoning include reduction during melting, fractional crystallization, accretion or condensation to the chondrule during crystallization, and the preservation of zoning profiles present in the precursor assemblage prior to melting. We agree with the reasoning of Matsunami *et al.* (1993) in eliminating Soret diffusion as a possible high-temperature process.

In order for any high-temperature process (above the chondrule solidus) to be able to create chemical zoning, it is necessary for at least one of several conditions to be met. Diffusion within the melt must be sufficiently slow that chemical gradients cannot homogenize, or melt in different parts of the chondrule could be physically separated, such as by being isolated between interlocking crystals. Alternatively, steep temperature gradients could exist across chondrules, for example, if only the outer part of a chondrule is melted while the inner part remains solid (as happens during coarse-grained rim formation; Rubin, 1984).

In the case where limited diffusion of species through a chondrule melt results in the preservation of chemical gradients, it would take a series of unlikely coincidences to produce the similar zoning profiles observed for many elements (constraint number (6), above). Although we know of no compilation of diffusion data appropriate for modeling chondrules for many elements, existing data at relevant temperatures and similar compositions indicate that different elements diffuse at vastly different rates. For example, Na diffuses much more rapidly than Ca near 1400 K in basaltic melts (Brady, 1995), which we calculate would lead to homogenization of Na gradients, but not Ca gradients over a length-scale of hundreds of microns if chondrules cooled at rates slower than ~1000 K/h (*e.g.*, Lofgren, 1996). It is possible that diffusion rates for various elements in chondrule glasses or melts could actually converge at very high temperatures (*e.g.*, Hart, 1981, who calculated convergence temperatures of ~1600 K for basaltic melts and ~3700 K for obsidian), but under these conditions and reasonable cooling rates, diffusion would be too extensive to allow preservation of zoning profiles. At lower temperatures, a wide variety of zoning profiles should develop for elements with different diffusion rates in a system with an initial compositional discontinuity for several elements (the case where chemically different material is added to the outside of a chondrule). Alternatively, different elements might enter a chondrule at different temperatures (*e.g.*, during condensation). Parallel zoning patterns might result if different elements had similarly sluggish diffusion rates in the melt just at their condensation temperatures. While this is conceivable, it seems extraordinarily unlikely for so many elements.

Because of this, high-temperature processes only seem appropriate for producing zoning in cases of physical isolation of mesostasis regions or strong temperature gradients. This implies that zoning trends can only be established at high degrees of crystallization or after secondary melting events. Simple models involving extensive melting of initially inhomogeneous material, or progressive condensation into high-temperature melts are excluded.

The Role of Reduction–In seven of eight zoned chondrules (including Matsunami's), Si and Al are inversely correlated, with the eighth case, 8-20, showing little variation in either element. But, in the two POP chondrules (7-24 and 1-2b), Si and Al are zoned in the opposite direction to the Matsunami chondrule, and Ca and Si show *correlated* zoning profiles (Fig. 7a), inconsistent with the Matsunami *et al.* (1993) scenario for producing zoning of major elements, where an increase of normative SiO_2 in outer zones is caused by reduction of olivine. Dilution by SiO_2 should also result in anticorrelations between the two nonvolatile minor elements, Cr and Ti, with Si. This is true in all of the olivine-rich chondrules, including Matsunami's, but not in the two PP chondrules, 7-2 and 7-30, which are zoned in Si but not in Cr and only one of which shows the expected zoning of Ti. Clearly, something more complex is occurring than in the Matsunami *et al.* (1993) reduction model. While we have little doubt that some reduction took place during melting of many low-FeO chondrules (as evidenced by the occurrence of low-Ni metal in many of them), a different explanation for major element zoning trends in mesostasis is required.

One possibility is that reduction *did* cause the nonvolatile-element zoning patterns in olivine-rich chondrules like Matsunami's, and another process caused the zoning patterns in more pyroxene-rich chondrules. However, a simple calculation shows that SiO_2 dilution cannot be responsible for zoning patterns even in olivine-rich chondrules. For example, in the Matsunami chondrule, the total difference between core and outer zone mesostasis is only ~4 wt% SiO_2, which can not account for the ~20% (relative) change in Al_2O_3 and even larger changes in TiO_2 and Cr_2O_3 observed across the same zones of this chondrule.

Fractional Crystallization–The mineralogy of the zoned chondrules is relatively simple. The BO and PO chondrules, 8-20, 7-31, and Matsunami's, all crystallized olivine as the only phenocryst phase, and the remaining liquid then crystallized small amounts of aluminous diopside before quenching. Simple calculations based on our mineral compositions (Table 1) show that liquids isolated at different degrees of olivine crystallization would have variable Si/Al ratios, but Si and Al would always be positively correlated, and both of these elements would anticorrelate with Mg. Because Si *anticorrelates* with Al in mesostasis zoning profiles, and particularly because Mg shows the least variability of any element across chondrule mesostases, olivine fractionation cannot play a role in establishing zoning patterns.

Chondrules that contain phenocrysts of low-Ca pyroxene should also have crystallized olivine first, and at lower temperatures pyroxene crystallized as olivine reacted with liquid. Poikilitic textures such as in the PP chondrules 7-2 and 7-30 and in the outer, pyroxene-rich zones of POP chondrules 7-24 and 7x-1 are undoubtedly the result of this reaction. Because the peritectic reaction to form pyroxene removes excess SiO_2 from the melt:

$$Mg_2SiO_4 \text{ (forsterite)} + SiO_2 \rightarrow 2MgSiO_3 \text{ (enstatite)}$$
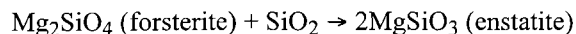
this might provide an explanation for the opposite Si-Al zoning behavior of POP chondrules compared with olivine-rich chondrules: residual melt trapped in the outer pyroxene-rich zone could be lower in Si and higher in Al (due to mass balance) than in the inner olivine-rich zone at an equivalent degree of Mg fractionation. The total core-to-rim change in mesostasis SiO_2 content across POP chondrules 1-2a and 7-24 is about 10–20%, which is similar to the range of Al_2O_3 contents, and consistent with this model. (This process could also cause minor enrichment of alkalis in pyroxene-rich outer zones, but nothing like the enrichments by factors of 8 and 4 observed for Na and K, respectively.)

The low-Ca pyroxene in POP chondrules is also rich in Cr_2O_3 (Table 1), affording a mechanism by which Cr could be removed from the liquid in the outer zone. Unfortunately, low-Ca pyroxene crystallization offers no mechanism by which Ca and Ti could become depleted in the outer zones: unlike Cr, these elements are not as strongly partitioned into this phase (compare Tables 1 and 2); Ca and Ti should actually rise, not fall, in the outer zones by this mechanism. Furthermore, even if this mechanism can account for Si, Al, and Cr zoning features of POP chondrules, it cannot play a role in BO and PO chondrules because they lack low-Ca pyroxene, and it is also unlikely to be important in PP chondrules such as 7-2 and 7-30, where there is no olivine-rich zone providing mineralogical contrast.

Late-stage crystallization of aluminous diopside (referred to below as CPX) is another igneous process that might fractionate chondrule mesostases. Relative to surrounding mesostasis, CPX is enriched in Ca, Ti, and Cr, and Mn, with apparent crystal–liquid distribution ratios averaging 1.7, 2.1, 5.7, and 1.6, respectively, in reasonable agreement with values measured by Jones and Scott (1989). A small amount of CPX crystallization could significantly deplete the liquid in these elements in a crystallizing chondrule, especially Cr, without greatly changing major elements. CPX is inhomogeneously distributed in many zoned chondrules, enhancing its ability to cause variable fractionations within chondrules. It tends to form overgrowths on low-Ca pyroxene, and thus has somewhat higher abundance in the outer shells of the POP chondrules. CPX also crystallized preferentially near the surface of BO chondrule 8-20, and may have even nucleated on the surface of this chondrule. PP chondrules show no preferential siting of CPX.

For chondrule 8-20, we calculated the effect that CPX crystallization would have on mesostasis composition, assuming that the starting composition was that of the mesostasis in the chondrule core (Table 2), and that CPX with our measured composition (Table 1) was removed. Several elements could be reasonably modeled in this way (Table 4). The best match between measured and calculated outer mesostasis composition was achieved with the removal of

TABLE 4. Calculation of the effect of aluminous diopside crystallization on the mesostasis composition of chondrule 8-20 (barred olivine).*

	Na_2O (wt%)	MgO (wt%)	Al_2O_3 (wt%)	SiO_2 (wt%)	CaO (wt%)	TiO_2 (wt%)	Cr_2O_3 (wt%)	MnO (wt%)
Aluminous diopside	0.09	13.5	18.3	45.9	21.6	1.23	0.80	0.11
Core mesostasis	0.16	9.8	23.1	48.0	18.6	1.00	0.36	0.10
Calculated outer mesostasis	0.20	7.9	25.6	49.0	17.0	0.88	0.13	0.09
Measured outer mesostasis	1.40	10.2	24.0	51.0	14.0	0.40	0.19	0.08

*The calculated outer mesostasis is the result of removing 34 wt% aluminous diopside from the core mesostasis.

~34 wt% CPX from the core mesostasis. In the model, Na, Al and Si rise, as observed in the actual outer mesostasis, and Ca, Ti, Cr, and Mn all decrease, also as observed (*e.g.*, Figs. 2 and 7b). Magnesium decreases in the model whereas it actually stays fairly constant in the chondrules. For elements that move in the right direction, the magnitudes of calculated fractionations do not perfectly match the actual chondrule data: Na does not rise nearly enough in the calculated outer zone; Al increases far too much; Si, Ti, and Mn do not change enough; and Cr is fairly well matched. Unfortunately, it is not reasonable to crystallize 34 wt% CPX to achieve these fractionations, as chondrule 8-20 has, in reality, no more than ~5 wt% CPX present in its outer zone. One solution to this discrepancy might be that we only were able to analyze the cores of coarse CPX grains, >10 μm across. Jones (1994) showed that Ca-pyroxene grains in some low-FeO chondrules are strongly zoned, with Ca-, Ti-, and Al-rich margins. If the same were true for chondrule 8-20, or if tiny CPX grains are more enriched in these elements than coarse grains, then much less CPX fractionation might be required, and the magnitude of calculated zoning profiles for Ca, Ti and Mn might more closely approach the actual values.

Further evidence that CPX crystallization might be important in the production of zoning profiles comes from the two PP chondrules, which have no mineralogical zoning of either CPX or low-Ca pyroxene. Correspondingly, they show no zoning of Cr, and little zoning of Ti and Mn in their mesostases. Nevertheless, their alkali, Ca, Al and Si zoning profiles require some other explanation.

The effect of CPX crystallization on the POP chondrules is more difficult to model quantitatively, as these chondrules may have also experienced some internal fractionation due to low-Ca pyroxene formation (see above). It seems reasonable that the decreases in Ca, Cr and Ti in mesostasis in the outer zones of these chondrules might be somehow related to higher CPX abundances in their low-Ca pyroxene-rich shells, but the difference in modal CPX between core regions and these shells is not as great as between inner and outer mesostasis in chondrule 8-20. Although CPX formation may have played a role in POP zoning, it cannot by any means explain all of the data.

In summary, there do seem to be some aspects of chondrule zoning that may have been caused or affected by fractional crystallization. In particular, these are the Si-Al zoning trend in POP chondrules, and decreases in Cr and Ti, and, in some cases, Ca and Mn in outer areas of mesostasis. However, with the exception of Mn, none of the volatile element zoning patterns can be explained in this way, nor can most of the zoning behavior of the major elements Al and Si.

Addition of Material at High Temperature–The low-FeO zoned chondrules studied here, plus the chondrule from Matsunami *et al.* (1993), form a chemical and mineralogical sequence going from BO + PO to POP to PP textures. Refractory element concentrations (Al, Ca, and Ti) decrease monotonically in mafic minerals and the more volatile elements (Fe, Mn and Cr) increase (Table 1) as the amount of modal pyroxene increases. Core mesostasis compositions show similar trends for the same elements, with alkalis in mesostasis following Fe, Mn and Cr in mafic phases. There are several plausible ways of explaining these trends. Sears *et al.* (1996) concluded that the group A2 → A1 transition (our PP chondrules are group A2 and our POP, PO, and BO chondrules are A1) was accomplished by increasing degrees of reduction and volatile loss from a ferroan precursor. Group A2 chondrules would have experienced extensive FeO reduction, giving rise to a highly enstatite-normative liquid, and loss of alkalis by evaporation. Group A1 chondrules would have begun to lose Si by evaporation, giving them highly forsterite-normative compositions and even lower amounts of alkalis and FeO than group A2. An alternative explanation is a model advocated in general by Rubin *et al.* (1999), and specifically by Krot *et al.* (2000a,b,c), in which chondrules may form sequentially from nebular condensates as temperature drops. The more refractory-rich, volatile-poor, olivine-rich chondrules would represent formation at higher temperature than the pyroxene-rich chondrules. Both of these models offer the opportunity for depositing low-temperature material around refractory chondrules. In the first model, volatiles could recondense and coat newly-formed chondrules upon cooling. In the second model, progressive condensation could deposit a lower temperature fraction of material on chondrules that formed at relatively higher temperature. In either case, elements deposited on a solid chondrule's surface might diffuse into chondrule mesostasis (considered in the next section of the discussion), or a secondary melting event could create a new

igneous layer of different composition mantling the original chondrule core. It may even be possible to condense or recondense material directly onto partially molten chondrules, as envisioned by Nagahara *et al.* (1999) and Tissandier *et al.* (2000).

There do not appear to be any unusual surface coatings on the zoned Semarkona chondrules, either in the form of coarse-grained rims or silica-rich rims. Chondrules 1-2a, 7-24, 7-31, 7x-1, and the Matsunami chondrule (all olivine-rich) have FeS-rich rims, but x-ray mapping reveals no unusual enrichments of elements other than S and Fe in these rims or in surrounding matrix. Pyroxene-rich chondrules 7-2 and 7-30, irregularly zoned chondrule 3-3a (PO), and 8-20 (BO) are surrounded only by matrix of typical composition. So, unless secondary melting events have caused mantles to be assimilated into the chondrules, there does not seem to be any evidence for accretion of significant amounts of lower temperature material around zoned chondrules.

However, there may be some evidence for late addition of material to some zoned chondrules. Chondrule 7-31 has a coarse outer mantle of olivine, poor in mesostasis, surrounding a fairly typical BO-textured core (Fig. 1); this may represent a case where solids accreted to an existing BO chondrule and were later melted around the outside. Low-FeO POP chondrules like 7-24, 7x-1 and 1-2b have always been mysterious in that there is no obvious reason why low-Ca pyroxene should form shells around olivine-rich cores. If millimeter-sized chondrules cooled at rates as slow as widely believed (<1000 K/h), they should be nearly internally isothermal throughout their cooling history, and olivine everywhere in the droplet should react with the melt when the pyroxene peritectic temperature is reached. One way to avoid this paradox could be to add SiO_2 and perhaps other nonrefractory elements by condensation into a silica-undersaturated chondrule while it was crystallizing olivine (*e.g.*, Tissandier *et al.*, 2000). The effect of this would be to lower the liquidus temperature, and olivine on the outside would begin to re-dissolve. If the olivine-rich core of the chondrule could not equilibrate with the now more completely molten exterior, then upon cooling the outside of the chondrule would eventually crystallize the poikilitic pyroxene shell.

Are the mineralogical data and zoning patterns of zoned chondrules consistent with addition of silicate material by secondary melting or direct condensation? To evaluate this, we calculated the bulk composition of the inner and outer portions of each chondrule by combining silicate phases in proportion to their modal abundances. Both BO chondrules have refractory-rich cores and outer zones that are much richer in moderately volatile elements (Fig. 8a,b). Elements of intermediate volatility, Mg, Cr, and Mn, show little fractionation from Si between core and outer zones. The difference between BO chondrule 7-31, which shows evidence for a secondary melting event, and 8-20, which has a very simple texture (cf., Fig. 1 of Connolly and Hewins, 1996), is that the refractories are somewhat fractionated in the outer zone of 8-20 compared

to 7-31. The behavior of Mg, Si, Cr, and Mn as a group in all zones of the BO chondrules is not what one would expect from recondensation or fractional condensation processes except under extraordinary circumstances, especially considering that their interelement ratios differ in the two chondrules. During evaporation of chondrules (the Sears model) and during progressive condensation of major elements like Si, ratios between elements like Mg and Si should not be constant (*e.g.*, Hashimoto, 1983; Petaev and Wood, 1998), including in liquids in equilibrium with gas at high dust/gas ratios (Ebel and Grossman, 2000). The mantle and core of 7-31 are more likely to be cogenetic: olivine and CPX are identical in composition in both zones, and much of the low refractory-element content of the mantle may simply be due to inhomogeneous distribution of mesostasis within the object (for unknown reasons).

SiO_2-addition models at high temperature to explain pyroxene shells around POP chondrules also do not seem entirely plausible. When core and outer areas of these chondrules are considered separately (Fig. 8c,d), both zones are calculated to have similar Al/Si ratios (near 1× the LL ratio), while the Mg/Si ratio is 2 × LL in the olivine-rich cores. Thus Mg/Si behaves as predicted by SiO_2 addition but Al/Si does not. The outer zones also show nonsolar Ca/Al ratios (as did the outer zone of 8-20), which are not easily explained by condensation or evaporation/recondensation models.

Finally, the compositions of the outer zones of PP chondrules do show a small amount of refractory element depletion compared to the inner zones, but virtually no Mg-Si-Cr-Mn fractionations are present (Fig. 8e,f). For similar reasons to those outlined above, and given the lack of any textural evidence, it is unlikely that secondary material was added to these chondrules by remelting.

Low- and Intermediate-Temperature Processes

Below the temperature at which chondrules were completely solidified (for the final time, in the case of multiple-melting events), two processes might result in zoned mesostasis. The first is solid-state diffusion of elements from chondrule exteriors into their glassy mesostasis, which would be favored at the highest possible temperature at which the glass remains solid due to the exponential dependence of diffusion rates upon temperature. The second process is introduction of elements *via* low-temperature chemical reactions involving hydration of glass during a period of aqueous alteration on the parent body. Because Semarkona has experienced essentially no asteroidal metamorphic heating these two processes do not represent a continuum: they would occur in very different settings. If elements diffused into chondrule glass at relatively high temperatures, it must have occurred while the chondrule was still warm, probably still in the environment in which chondrules are forming, and on a timescale appropriate to such a setting.

Diffusion into Warm Chondrules–As chondrules cooled below the solidus temperature, volatile elements remaining in
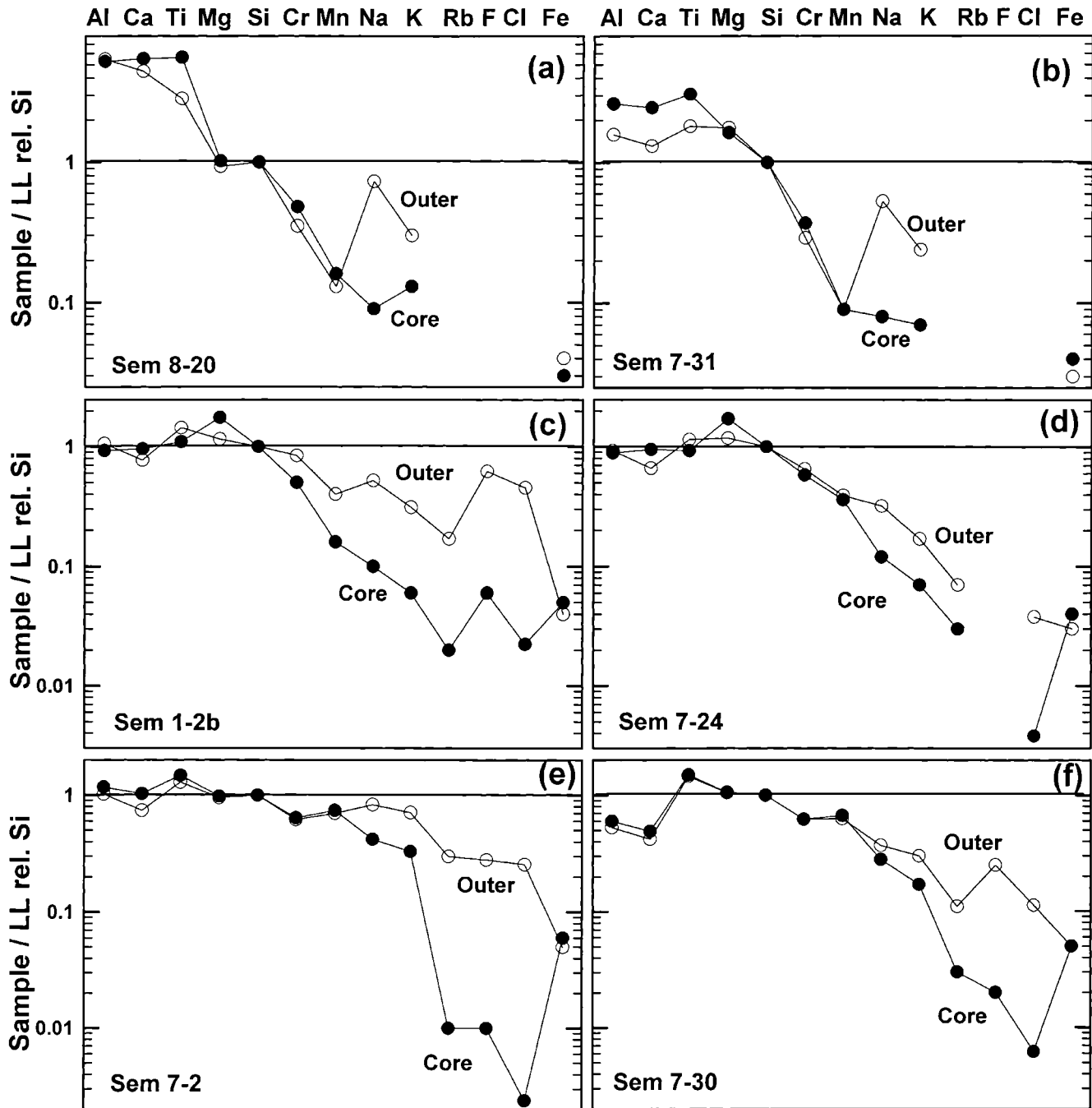
FIG. 8. Elemental abundance patterns calculated for bulk core and outer zones of zoned Semarkona chondrules. Bulk compositions were calculated based on modal analysis of phases in Mg x-ray maps, mean olivine and pyroxene compositions, and mean compositions of mesostasis in each part of the chondrule. The differences in abundance patterns for nonvolatile elements (Al through Cr) are not consistent with addition of condensates to the outer zones of the chondrules (note fractionations among refractories and relatively constant Mg/Si ratio). Moderately volatile elements are always higher in the outer zones.

the surrounding gas may have condensed onto surfaces and immediately begun to diffuse into the volatile-poor interiors (Matsunami *et al.*, 1993; Nagahara *et al.*, 1999). All elements that we observe to be uniformly enriched at chondrule surfaces (H, Na, K, Rb, F, and Cl) are considerably more volatile than the major elements. With the exception of H, these are

moderately volatile, with 50% condensation temperatures varying by >300 K, from 736 K (F) up to ~1080 K (Rb) in a gas of solar composition at 10^{-4} atm (Wasson, 1985). These temperatures are probably, for the most part, below that at which chondrules solidified (<1100 K; Gooding, 1979), although condensation temperatures for alkalis and, presumably, other

elements can rise by several 100 K in systems with a large amount of vaporized solids (e.g., Ebel and Grossman, 2000). While there is no literature source for diffusion parameters for all of these elements in glass with compositions appropriate to chondrules, it is reasonable to assume that there will be a large amount of variation. For example, at 1000 K, self-diffusion coefficients for Na, K, and Rb in obsidian glass are ~5 × 10⁻⁷, 1 × 10⁻⁸, and 3 × 10⁻¹⁰ cm² s⁻¹, respectively (Jambon, 1982), corresponding to a 40-fold variation in diffusion length-scales among these elements. In light of this, it is extremely unlikely that the observed families of parallel zoning profiles in chondrule mesostases could be produced by simple diffusion through glass.

Calcium zoning profiles would also be difficult to produce in the environment where chondrules formed. Most of the Ca variation in zoned chondrules cannot be explained by igneous fractionation. In every case, Ca is depleted in mesostasis near chondrule surfaces where volatiles are enriched, strongly suggesting that all of these elements are coupled. Calcium would have to be diffusing out to chondrule surfaces and then evaporating while volatiles were condensing, a behavior not in keeping with the predicted highly refractory nature of Ca under most conditions. Without a strong sink for Ca, which is difficult to imagine in the region of chondrule formation, we cannot see any way to explain Ca zoning in this model.

Aqueous Alteration–Although it is possible that H entered chondrules at much lower temperature than alkalis and other volatiles, and that the correlation between H_2O and the other elements is just a coincidence, it is clearly worth considering whether aqueous processes on the parent body may have introduced H_2O and some other elements together during the same event. The fact that volatile elements with a wide range of condensation temperatures are all enriched in outer zones of chondrules, whereas elements such as Ca and, perhaps, other major and minor elements have moved out of chondrules should be much easier to explain if chondrules were in direct contact with potential sources and sinks for these elements in a parent-body setting rather than when the chondrules were isolated from other solids in a gas. For such a model to be correct, it must be possible to aqueously alter glass without devitrifying it. The model must also overcome the major shortfall of most of the high-temperature models: zoning profiles produced by the process for many elements must be generally parallel.

It is possible to hydrate and chemically alter igneous glass without devitrification. Mungall and Martin (1994) reported an extreme example in which trachytic glass was hydrated and leached of large fractions of many elements while remaining optically isotropic and without displaying x-ray diffraction peaks. This paper also cites a variety of other studies related to the leaching of natural glass by aqueous solutions without devitrification. Most of the elemental mobility documented in these studies involves the removal of components (leaching) from the glass during hydration. However, in the Mungall and Martin (1994) study, Sr was greatly enriched in the glass as

other elements were lost. They suggested a mechanism by which the glass structure is modified during influx of water and Na^+–H^+ exchange, essentially opening it to the free diffusion of many cations, which can then equilibrate rapidly with the fluid.

A mechanism such as suggested by Mungall and Martin (1994) has obvious appeal for the problem of chondrule zoning. If the extent of glass hydration, measured as the H_2O content by ion probe, controls the rates at which elements can diffuse, then the zoning of other elements could follow that of H_2O. But there are great uncertainties as to whether this mechanism can be applied. None of the chondrule mesostases has a water content approaching the 4–7 wt% range of glasses studied by Mungall and Martin (1994), and we do not know how much hydration is necessary to enhance elemental mobility. The glass and, presumably, fluid compositions are different in the terrestrial and chondritic systems, adding further complications.

If such a mechanism can result in alteration of glasses in chondrules without devitrification, there is no problem in identifying the sources and sinks for the most mobile elements. Aqueous fluids on the parent body would easily flow through and exchange with porous matrix and rim material, which would be an excellent source for moderately volatile elements like alkalis and halogens (e.g., Grossman, 1985; Alexander, 1995). The high solubility and mobility of Ca during aqueous alteration is evident from studies of altered mesostasis in chondrules in CM chondrites (Richardson, 1981; Ikeda, 1983; Hanowski and Brearley, 2001). In almost all cases, Ca has been entirely removed and has been reprecipitated as calcite elsewhere in the chondrite. A very similar process probably occurred in Semarkona, but to a much more limited extent that resulted in the formation of a limited amount of calcite (Hutchison et al., 1987). But we do not know whether exchange between chondrule glass and matrix during aqueous alteration could explain the zoning profiles of Si, Al, and other elements in chondrules where igneous models fall short.

Deuterium/Hydrogen Ratios

Three of four measured zoned chondrules show a correlation between δD and H_2O (and other volatile element) content in mesostasis, suggesting multi-component mixing of sources with different H isotopic composition. Given the very low content of moderately volatile elements in the cores of the zoned chondrules, which are <0.01 × bulk LL in some cases (Fig. 8), we would expect that the original core H_2O content would most likely have been much less than the minimum measured values of 100–200 ppm; H_2O was probably introduced into the cores by a secondary process. In our previous work on bleached chondrules in Semarkona (Grossman et al., 2000), we found that contamination by terrestrial water can be a serious problem in hydrogen isotopic measurements of chondrules, and it is possible that there is a low δD, terrestrial water component mixed in with any or all

of our analyses to varying degrees. Whether the low δD H_2O component is terrestrial or not, the outer parts of zoned chondrules are clearly dominated by an extraterrestrial, high δD component. With δD reaching values of up to +2300‰, we interpret this to be water of hydration that equilibrated with surrounding matrix, which is known to be D-rich (Deloule and Robert, 1995; Grossman *et al.*, 2000).

Origin of Cathodoluminescence Zoning

Although none of the present chondrules shows as broad a ring of bright yellow luminescent mesostasis as does the Matsunami *et al.* (1993) chondrule, neither do any have as broad an alkali-enriched zone as the Matsunami chondrule. This, and the correlation in individual chondrules of thermoluminescence (TL) with Na abundance, support the idea that the process responsible for CL zoning is related to the process that caused alkali enrichment. We find no mineralogical or physical evidence to suggest that the phenomena observed by Matsunami *et al.* (1993) and by us are not one and the same.

Matsunami *et al.* (1993) attributed zoning in CL as well as induced TL in their chondrule to Mn, which increased monotonically toward the chondrule edge along with Na. They observed that Mn^{2+} substitution for Ca^{2+} in calcic feldspar produces a similar TL spectrum to that in the chondrule, and that Mn rises by a similar factor to TL intensity near the edge of the chondrule. In an experimental study, DeHart and Lofgren (1996) found that precipitation of diopside during late stages of crystallization of low-FeO chondrules, which increases residual liquids in normative anorthite, is necessary to produce the characteristic yellow CL. In these experiments, aqueous alteration destroyed yellow CL.

Four olivine-rich, concentrically zoned chondrules studied here all show CL zoning, from relatively bright yellow on the edge, to dull yellow in the cores. Three of these chondrules show Mn zoning like the Matsunami chondrule, but the absolute levels of Mn in the mesostasis are variable. For example, 8-20 has less Mn in its bright-yellow luminescing outer region than 7-24 does in its barely luminescent core. The fourth chondrule with zoned CL, 7-31, has uniformly low Mn. The PP chondrule with uniformly high Mn in mesostasis, 7-30, shows mostly uniform, dull-yellow CL. Clearly, yellow CL intensity is not a simple function of Mn concentration. Rather, the important factor is probably the abundance of the Mn-bearing phosphor in the mesostasis, possibly a calcic feldspar component as suggested by Matsunami *et al.* (1993). Hydration of glass does not seem to have destroyed yellow CL, unlike in the DeHart and Lofgren (1996) study, probably because the conditions of alteration in Semarkona were much less severe than in the laboratory experiments, and no devitrification occurred. In fact, the very bright CL at the edge of the most H_2O-rich chondrule, 1-2b, suggests that light aqueous alteration may actually play a role in enhancing yellow CL, perhaps because of structural changes in glass that accompany hydration.

Irregularly Zoned Chondrules

We only examined a single case of an irregularly zoned chondrule. 3-3a has alkali enrichments both near its edge and around coarse olivine phenocrysts. As it shares many chemical properties with concentrically zoned low-FeO chondrules, we would suggest that the zoning in all of these chondrules has the same origin. Perhaps in this chondrule there were pathways along grain boundaries or cracks that allowed fluids access to the interior. Or, given the small size of 3-3a, it is possible that the thin section mainly passed through the outer zone, greatly exaggerating its thickness as well as minor irregularities in its zonation.

The Origin of High-Sodium Chondrules

Given that low-FeO chondrules in Semarkona commonly show zoning trends in alkalis and other moderately volatile elements, it is worth considering whether similar processes to those that caused this zoning may have gone to completion in uniformly volatile-rich chondrules. Chondrule 7-5 is a relatively uncommon type of chondrule (<15% of low-FeO chondrules) in that it is quite low in FeO (Fa_4 olivine), yet is very rich in Na (mesostasis contains ~80 wt% normative albite). In most of the compositional diagrams presented in Figs. 5 and 6, chondrule 7-5 lies along extrapolations of zoning trends in individual chondrules. Thus, a strong case can be made that this type of object is a fully metasomatized chondrule, far in composition from its primary state.

Most alkali-rich chondrules, however, are not low in FeO. These are dominated by the type II or group B chondrules, which have different bulk and mesostasis compositions from low-FeO chondrules: they are richer in silica and poorer in refractories in addition to being high in FeO and volatiles, and mesostases are generally higher in normative quartz as well as albite. In Fig. 9, the mesostasis trends for the alkalis, Na and K, in zoned low-FeO chondrules from the present work are superimposed on datasets taken from random Semarkona chondrules. Shown are unpublished mesostasis analyses done by the first author, using the methods described above, on 14 chondrules with Fa_{10} olivine or higher from section USNM 1805-7. Also shown are bulk instrumental neutron activation analysis (INAA) data on 12 separated porphyritic chondrules with Fa_{10} or higher analyzed by Grossman and Wasson (1983, 1985). Bulk data can be compared to EPMA data in this way because Na, K, and the normalizing element Al are nearly entirely contained in mesostasis. Zoning patterns within individual low-FeO chondrules all follow trajectories with lower-than-solar K/Na ratios, passing through a few, unusual, low-alkali, ferroan chondrules. In their outermost zones, the two zoned PP chondrules, 7-2 and 7-30, become more K-rich, and follow the same trend as ferroan chondrules toward alkali-rich compositions with superchondritic K/Na. All low-FeO chondrules in the same INAA and random-chondrule datasets (not plotted) overlie the zoned-chondrule trends in Fig. 9.
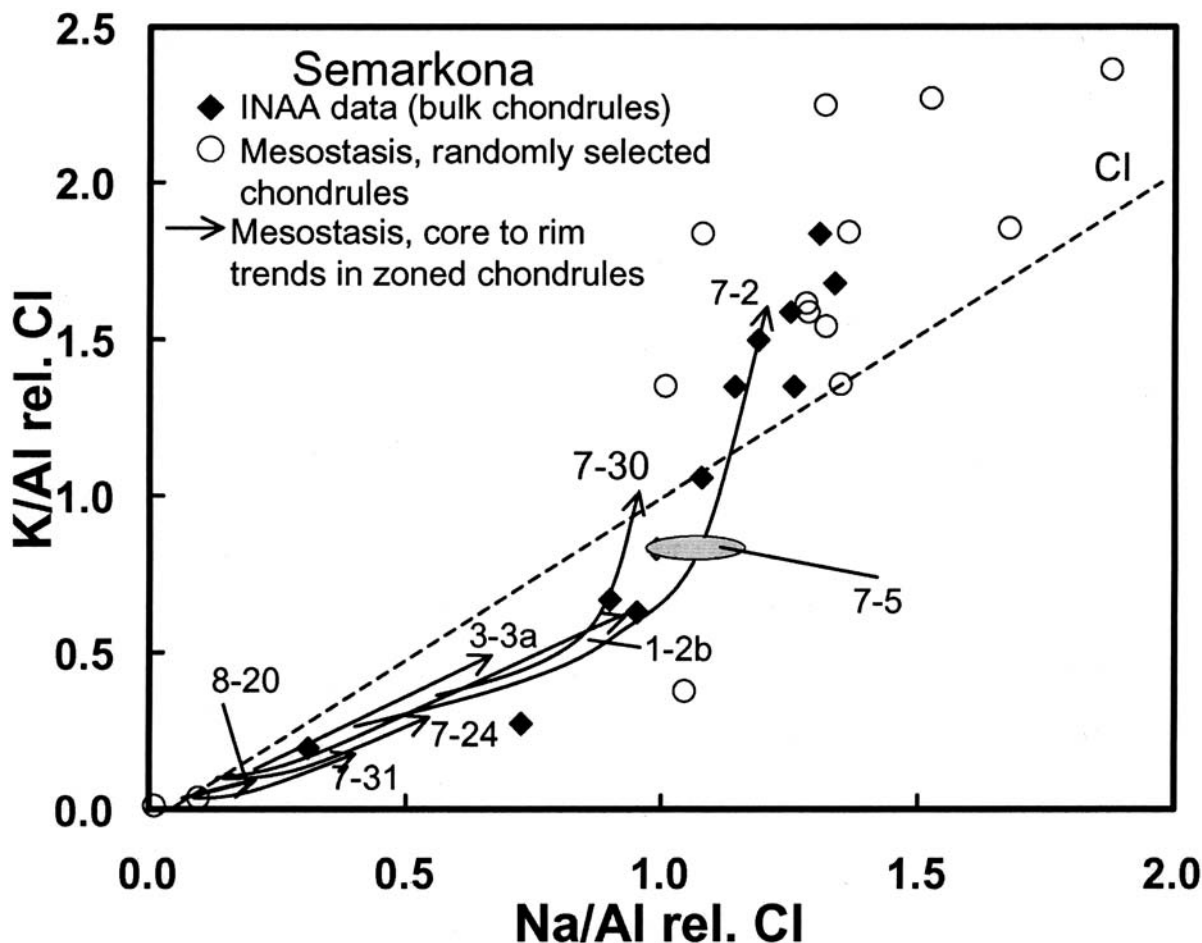
FIG. 9. Na and K relationships in zoned chondrule mesostases, compared to mesostases in randomly selected high-FeO chondrules (circles) and bulk INAA analyses of high-FeO chondrules. Data are normalized to Al and to CI chondrites. Zoned low-FeO chondrules show trends on this diagram that are very similar to those shown by seemingly unrelated high-FeO chondrules, suggesting that similar processes operated on each type.

The data in Fig. 9 are highly suggestive of a link between the process that introduced alkalis into zoned chondrules with the process resulting in uniformly high alkalis in ferroan chondrules. However, the alkali enrichment trends in low-FeO chondrules are *not* associated with FeO-enrichment, and thus there is no reason to think that low-FeO chondrules could somehow evolve into high-FeO ones *via* metasomatism and remelting. But it is worth considering whether the mesostasis in high-FeO chondrules may not be primary in composition. We will not speculate on this question any further here; but new work on high-FeO chondrule mesostasis indicates that it does not always have compositions indicative of simple igneous processes (Grossman, 2000).

CONCLUSIONS

Radial zonation of mesostasis is a fairly common phenomenon in low-FeO chondrules from Semarkona. There is good evidence that both high- and low-temperature processes

were involved in the creation of zoned chondrules; no simple model can explain all of their properties.

The large enrichments of moderately volatile elements and water that occur in the outer portions of these chondrules are far greater in magnitude than can be produced by primary igneous processes. We suggest that one possible cause for these enrichments is hydration of glass during a period of light aqueous alteration on the parent asteroid. This process essentially opened the glass structure to the rapid diffusion and exchange of elements with surrounding matrix and rim material. During this process, volatile elements entered the initially volatile-poor glass, and Ca was leached out of the chondrules. Evidence from terrestrial systems suggests that this process can indeed occur without devitrification of the glass.

Smaller enrichments and depletions of nonvolatile major and minor elements, exclusive of Mg and Fe, accompany the enrichment of moderately volatile elements and water in zoned chondrules. In some cases, it appears that preferential crystallization of low- and, especially, high-Ca pyroxene near the chondrule

surface, coupled with lack of equilibration of residual liquid across the chondrule, might have played a role in creating zoned mesostasis. Differences in Si, Al, and Cr zoning between POP and PO/BO/PP chondrules may have been affected by low-Ca pyroxene crystallization, whereas high-Ca pyroxene crystallization might have played a role in the creation of Ti, Cr, and Mn zoning.

All other models for production of zoning profiles while chondrules were still warm or hot, either before solidification or during cooling in the chondrule-formation region, seem to have serious deficiencies. Abundance patterns in outer zones of chondrules are inconsistent with progressive condensation models, either directly into chondrule melts or onto chondrule surfaces. All high-temperature models suffer from the inability to produce families of sub-parallel zoning patterns due to widely ranging diffusion rates of different elements.

REFERENCES

ALEXANDER C. M. O'D. (1995) Trace element contents of chondrule rims and interchondrule matrix in ordinary chondrites. *Geochim. Cosmochim. Acta* 59, 3247–3266.

ALEXANDER C. M. O'D., BARBER D. J. AND HUTCHISON R. H. (1989) The microstructure of Semarkona and Bishunpur. *Geochim. Cosmochim. Acta* 53, 3045–3057.

ARMSTRONG J. T. (1995) CITZAF: A package of correction programs for the quantitative electron microbeam x-ray analysis of thick polished materials, thin films, and particles. *Microbeam Anal.* 4, 177–200.

BISCHOFF A. (1998) Aqueous alteration of carbonaceous chondrites: Evidence for preaccretionary alteration—A review. *Meteorit. Planet. Sci.* 33, 1113–1122.

BRADY J. B. (1995) Diffusion data for silicate minerals, glasses, and liquids. In *Mineral Physics and Crystallography: A Handbook of Physical Constants* (ed. T. J. Ahrens), pp. 269–290. American Geophysical Union, Washington, D.C., USA.

BRIDGES J. C., ALEXANDER C. M. O'D., HUTCHISON R., FRANCHI I. A. AND PILLINGER C. T. (1997) Sodium-, chlorine-rich mesostases in Chainpur (LL3) and Parnallee (LL3) chondrules. *Meteorit. Planet. Sci.* 32, 555–565.

CONNOLLY H. C. AND HEWINS R. H. (1996) Constraints of chondrule precursors from experimental data. In *Chondrules and the Protoplanetary Disk* (eds. R. H. Hewins, R. H. Jones and E. R. D. Scott), pp. 129–135. Cambridge Univ. Press, Cambridge, U.K.

DEHART J. M. AND LOFGREN G. (1996) Experimental studies of group A1 chondrules. *Geochim. Cosmochim. Acta* 60, 2233–2242.

DELOULE E. AND ROBERT F. (1995) Interstellar water in meteorites? *Geochim. Cosmochim. Acta* 59, 4695–4706.

DODD R. T. (1971) The petrology of chondrules in the Sharps meteorite. *Contrib. Mineral. Petrol.* 31, 201–227.

EBEL D. S. AND GROSSMAN L. (2000) Condensation in dust-enriched systems. *Geochim. Cosmochim. Acta* 64, 339–366.

GOODING J. L. (1979) Petrogenetic properties of chondrules in unequilibrated H-, L-, and LL-group chondritic meteorites. Ph.D. dissertation thesis, Univ. New Mexico, Albuquerque, New Mexico, USA. 392 pp.

GROSSMAN J. N. (1985) Chemical evolution of the matrix of Semarkona (abstract). *Lunar Planet. Sci.* 17, 1302–1303.

GROSSMAN J. N. (2000) Concentric zoning of phosphorus and bimodal alkali contents of mesostasis in type II chondrules. (abstract). *Lunar Planet. Sci.* 31, #1599, Lunar and Planetary Institute, Houston, Texas, USA (CD-ROM).

GROSSMAN J. N. AND WASSON J. T. (1983) Refractory precursor components of Semarkona chondrules and the fractionation of refractory elements among chondrules. *Geochim. Cosmochim. Acta* 47, 759–771.

GROSSMAN J. N. AND WASSON J. T. (1985) The origin and history of the metal and sulfide components of chondrules. *Geochim. Cosmochim. Acta* 49, 925–939.

GROSSMAN J. N., ALEXANDER C. M. O'D., WANG J. AND BREARLEY A. J. (2000) Bleached chondrules: Evidence for widespread aqueous processes on the parent asteroids of ordinary chondrites. *Meteorit. Planet. Sci.* 35, 467–486.

HANOWSKI N. P. AND BREARLEY A. J. (2001) Aqueous alteration of chondrules in the CM carbonaceous chondrite, Allan Hills 81002: Implications for parent body alteration. *Geochim. Cosmochim. Acta* 65, 495–518.

HART S. R. (1981) Diffusion compensation in natural silicates. *Geochim. Cosmochim. Acta* 45, 279–291.

HASHIMOTO A. (1983) Evaporation metamorphism in the early solar nebula: Evaporation experiments on the melt $FeO-MgO-SiO_2-CaO-Al_2O_3$ and chemical fractionations of primitive materials. *Geochem. J.* 17, 111–145.

HUTCHISON R., ALEXANDER C. M. O'D. AND BARBER D. J. (1987) The Semarkona meteorite: First recorded occurrence of smectite in an ordinary chondrite, and its implication. *Geochim. Cosmochim. Acta* 51, 1875–1882.

HUTCHISON R., ALEXANDER C. M. O'D. AND BRIDGES J. C. (1994) Chlorine metasomatism and elemental redistribution in unequilibrated ordinary chondrites (abstract). *Meteoritics* 29, 476–477.

IKEDA Y. (1983) Alteration of chondrules and matrices in the four Antarctic carbonaceous chondrites ALH-77307 (C3), Y-790123 (C2), Y-75293 (C2) and Y-74662 (C2). *Mem. Natl. Inst. Polar Res., Spec. Issue* 30, 93–108.

IKEDA Y. AND KIMURA M. (1995a) Anhydrous alteration of Allende chondrules in the solar nebula I: Description and alteration of chondrules with known oxygen-isotopic compositions. *Proc. NIPR Symp. Antarct. Meteorites* 8, 97–122.

IKEDA Y. AND KIMURA M. (1995b) Anhydrous alteration of Allende chondrules in the solar nebula II: Alkali-Ca exchange reactions and formation of nepheline, sodalite and Ca-rich phases in chondrules. *Proc. NIPR Symp. Antarct. Meteorites* 8, 123–138.

JAMBON A. (1982) Tracer diffusion in granitic melts. *J. Geophys. Res.* 87, 10 797–10 810.

JONES R. H. (1994) Petrology of FeO-poor, porphyritic pyroxene chondrules in the Semarkona chondrite. *Geochim. Cosmochim. Acta* 58, 5325–5340.

JONES R. H. AND SCOTT E. R. D. (1989) Petrology and thermal history of type IA chondrules in the Semarkona (LL3.0) chondrite. *Proc. Lunar Planet. Sci. Conf.* 19th, 523–536.

KROT A. N., SCOTT E. R. D. AND ZOLENSKY M. E. (1995) Mineralogical and chemical modification of components in CV3 chondrites: Nebular or asteroidal processing? *Meteoritics* **30**, 748–775.

KROT A., SCOTT E. R. D. AND ZOLENSKY M. (1997a) Origin of fayalitic olivine rims and lath-shaped matrix olivine in the CV3 chondrite Allende and its dark inclusions. *Meteorit. Planet. Sci.* **32**, 31–49.

KROT A. N., ZOLENSKY M. E., WASSON J. T., SCOTT E. R. D., KEIL K. AND OHSUMI K. (1997b) Carbide-magnetite assemblages in type-3 ordinary chondrites. *Geochim. Cosmochim. Acta* **61**, 219–237.

KROT A. N., MEIBOM A. AND KEIL K. (2000a) Volatile-poor chondrules in the CH carbonaceous chondrites: Formation at high nebular temperature (abstract). *Lunar Planet. Sci.* **31**, #1481, Lunar and Planetary Institute, Houston, Texas, USA (CD-ROM).

KROT A. N., MEIBOM A., RUSSELL S. S., YOUNG E., ALEXANDER C. M., MCKEEGAN K. D., LOFGREN G., CUZZI J., ZIPFEL J. AND KEIL K. (2000b) Chondrules of the very first generation in Bencubbin/CH-like meteorites QUE 94411 and Hammadah al Hamra 237: Condensation origin at high ambient nebular temperatures (abstract). *Lunar Planet. Sci.* **31**, #1499, Lunar and Planetary Institute, Houston, Texas, USA (CD-ROM).

KROT A. N., WEISBERG M. K., PETAEV M. I., KEIL K. AND SCOTT E. R. D. (2000c) High-temperature condensation signatures in type I chondrules from CR carbonaceous chondrites (abstract). *Lunar Planet. Sci.* **31**, #1470, Lunar and Planetary Institute, Houston, Texas, USA (CD-ROM).

LOFGREN G. E. (1996) A dynamic crystallization model for chondrule melts. In *Chondrules and the Protoplanetary Disk* (eds. R. H. Hewins, R. H. Jones and E. R. D. Scott), pp. 187–196. Cambridge Univ. Press, Cambridge, U.K.

LYON I. C., SAXTON J. M., SEARS D. W. G., SYMES S. AND TURNER G. (1999) Possible mass-independent oxygen-isotopic fractionation in the mesostasis of a Semarkona group A1 chondrule (abstract). *Meteorit. Planet. Sci.* **34 (Suppl.)**, A76.

MAHARAJ S. V. AND HEWINS R. H. (1998) Chondrule precursor minerals as anhydrous phases. *Meteorit. Planet. Sci.* **33**, 881–887.

MATSUNAMI S., NINAGAWA K., NISHIMURA S., KUBONO N., YAMAMOTO I., KOHATA M., WADA T., YAMASHITA Y., LU J., SEARS D. W. G. AND NISHIMURA H. (1993) Thermoluminescence and compositional zoning in the mesostasis of a Semarkona group A1 chondrule and new insights into the chondrule-forming process. *Geochim. Cosmochim. Acta* **57**, 2101–2110.

MCCOY T. J., SCOTT E. R. D., JONES R. H., KEIL K. AND TAYLOR G. J. (1991) Composition of chondrule silicates in LL3-5 chondrites and implications for their nebular history and parent body metamorphism. *Geochim. Cosmochim. Acta* **55**, 601–619.

MUNGALL J. E. AND MARTIN R. F. (1994) Severe leaching of trachytic glass without devitrification, Terceira, Azores. *Geochim. Cosmochim. Acta* **58**, 75–83.

NAGAHARA H., KITA N. T., OZAWA K. AND MORISHITA Y. (1999) Condensation during chondrule formation: Elemental and Mg isotopic evidence (abstract). *Lunar Planet. Sci.* **30**, #1917, Lunar and Planetary Institute, Houston, Texas, USA (CD-ROM).

PALME H. AND FEGLEY B. (1990) High-temperature condensation of iron-rich olivine in the solar nebula. *Earth Planet. Sci. Lett.* **101**, 180–195.

PECK J. A. AND WOOD J. A. (1987) The origin of ferrous zoning in Allende chondrule olivine. *Geochim. Cosmochim. Acta* **51**, 1503–1510.

PETAEV M. I. AND WOOD J. A. (1998) The condensation with partial isolation (CWPI) model of condensation in the solar nebula. *Meteorit. Planet. Sci.* **33**, 1123–1137.

RICHARDSON S. M. (1981) Alteration of mesostasis in chondrules and aggregates in three C2 carbonaceous chondrites. *Earth Planet. Sci. Lett.* **52**, 67–75.

RUBIN A. E. (1984) Coarse-grained chondrule rims in type 3 chondrites. *Geochim. Cosmochim. Acta* **48**, 1779–1789.

RUBIN A. E., SAILER A. L. AND WASSON J. T. (1999) Troilite in the chondrules of type-3 ordinary chondrites: Implications for chondrule formation. *Geochim. Cosmochim. Acta* **63**, 2281–2298.

SCOTT E. R. D. AND TAYLOR G. J. (1983) Chondrules and other components in C, O, and E chondrites: Similarities in their properties and origins. *Proc. Lunar Planet. Sci. Conf.* **14th**, B275–B286.

SEARS D. W. G. AND AKRIDGE G. (1998) Nebular or parent body alteration of chondritic material: Neither or both? *Meteorit. Planet. Sci.* **33**, 1157–1167.

SEARS D. W. G., LU J., BENOIT P. H., DEHART J. M. AND LOFGREN G. E. (1992) A compositional classification scheme for meteoritic chondrules. *Nature* **357**, 207–210.

SEARS D. W. G. *ET AL.* (1995) Metamorphism and aqueous alteration in low petrographic type ordinary chondrites. *Meteoritics* **30**, 169–181.

SEARS D. W. G., HUANG S. AND BENOIT P. H. (1996) Open-system behavior during chondrule formation. In *Chondrules and the Protoplanetary Disk* (eds. R. H. Hewins, R. H. Jones and E. R. D. Scott), pp. 221–231. Cambridge Univ. Press, Cambridge, U.K.

SEARS D. W. G., LYON I. C., SAXTON J. M., SYMES S. AND TURNER G. (1999) Oxygen isotope heterogeneity in the mesostasis of a Semarkona group A1 chondrule (abstract). *Lunar Planet. Sci.* **30**, #1406, Lunar and Planetary Institute, Houston, Texas, USA (CD-ROM).

TAYLOR G. J., OKADA A., SCOTT E. R. D., RUBIN A. E., HUSS G. R. AND KEIL K. (1981) The occurrence and implications of carbide-magnetite assemblages in unequilibrated ordinary chondrites (abstract). *Lunar Planet. Sci.* **12**, 1076–1078.

TISSANDIER L., LIBOUREL G. AND ROBERT F. (2000) Experimental silica condensation and its bearing on chondrule formation (abstract). *Meteorit. Planet. Sci.* **35 (Suppl.)**, A156–A157.

WASSON J. T. (1985) *Meteorites: Their Record of Early Solar-System History.* Freeman, New York, New York, USA. 267 pp.

WASSON J. T. AND KALLEMEYN G. W. (1988) Compositions of chondrites. *Phil. Trans. Royal Soc. London* **A325**, 535–544.

WASSON J. T. AND KROT A. N. (1994) Fayalite-silica association in unequilibrated ordinary chondrites-evidence for aqueous alteration on a parent body. *Earth Planet. Sci. Lett.* **122**, 403–416.

WEINBRUCH S., PALME H., MÜLLER W. F. AND EL GORESY A. (1990) FeO-rich rims and veins in Allende forsterite: Evidence for high temperature condensation at oxidizing conditions. *Meteoritics* **25**, 115–125.